Johannes Kepler University Linz
Faculty of Engineering and natural Sciences

University of South Bohemia in České Budějovice
Faculty of Science

Late Steps in the cytosolic Iron-Sulfur Cluster Assembly in *Trypanosoma brucei*

Master thesis

Haindrich Alexander Christoph

Cross-Border joint Master's Program
Biological Chemistry

Supervisor: Priscila Peña Diaz, PhD.
Department of Molecular Biology
Institute of Parasitology, Biology Centre, Academy of Sciences of Czech Republic
and
Faculty of Science, University of South Bohemia

České Budějovice, 2015

Haindrich A. C., 2015. Late Steps in the cytosolic Iron-Sulfur Cluster Assembly in *Trypanosoma brucei*. MSc. thesis in English, 54 p, Faculty of Science, University of South Bohemia, České Budějovice, Czech Republic

Annotation

The aim of this thesis was to investigate genes involved in the late steps of the Cytosolic Iron sulfur cluster Assembly (CIA) pathway in procyclic *T. brucei*, to determine their cellular localization and find their possible interaction partners and substrates.

Annotation

Das Ziel dieser Arbeit war die Untersuchung von Genen involviert in der Schlussphase des cytosolischen Eisen Schwefel Cluster Syntheseweges in der prozyklischen trypomastigoten Form von *T. brucei*. Die zelluläre Lokalisierung der Proteine sollte bestimmt werden sowie nach möglichen Reaktionspartnern oder Substraten gesucht werden.

Affirmation

I hereby declare that, in accordance with Article 47b of Act No. 111/1998 in the valid wording, I agree with the publication of my bachelor thesis, in full to be kept in the Faculty of Science archive, in electronic form in publicly accessible part of STAG database operated by the University of South Bohemia in České Budějovice accessible through its web pages. Further, I agree to the electronic publication of the comments of my supervisor and thesis opponents and the record of the proceedings and results of the thesis defence in accordance with aforementioned Act. No. 111/1998. I also agree to the comparison of the text of my thesis with the Thesis.cz thesis database operated by the National Registry of University and a plagiarism detection system.

České Budějovice, 14. 12. 2015

.....

Alexander Haindrich

Sworn Declaration

I hereby declare under oath that the submitted Master's degree thesis has been written solely by me without any third-party assistance, information other than provided sources or aids have not been used and those used have been fully documented. Sources for literal, paraphrased and cited quotes have been accurately credited.
The submitted document here present is identical to the electronically submitted text document.

České Budějovice, 14. 12. 2015

.....

Alexander Haindrich

Acknowledgements

I would like to thank my supervisor Prof. Julius Lukeš for the opportunity to work in his lab, and his patience in the project although I had several drawbacks because of which I had to start all over again (several times).
I also express my gratitude to my former supervisor during my bachelor thesis, Somsuvro Basu, for leaving such a nice project in my hands and his strong faith in my capabilities to finish it. Also I would like to thank Eva Horáková as my group leader for her support in my experiments and her critical second opinion on interpretation of my results.
I am most grateful that I can call Priscila Peña Diaz as my supervisor during the work on my master thesis, for help in difficult decision and troublesome experimental set-ups, mental support when I ran out of ideas, and that I can call the imprint of her charming nature as part of my development as young scientist.
Finally I also thank my bachelor student Michala Boudová for the possibility to reflect on myself and her leniency on my occasional anarchic way of supervising her.

Abbreviations

BSA	bovine serum albumin
c-aconitase	cytosolic aconitase
CIA	cytosolic iron-sulfur cluster assembly
EPR	electron paramagnetic resonance
FBS	fetal bovine serum
Fe-S	iron-sulfur
HBSS	Hanks buffered saline solution
IFA	immunofluorescence assay
ISC	iron-sulfur cluster system
LECA	last eukaryotic common ancestor
NIF	nitrogen fixation system
PCR	polymerase chain reaction
PBS	phosphate buffered saline
RNAi	RNA interference
RT	room temperature
SAM	s-adenosylmethionine
SUF	sulfur utilization factor system
T. brucei	*Trypanosoma brucei*
TX-100	Triton X-100

Introductory note

The genes studied in this thesis are named mostly after their yeast or human orthologues. The following table should help as orientation on which gene is addressed if one of the stated names is used. The following genes have been studied:

Table 1: Summary of gene names of CIA components in *S. cerevisiae* and Human and their predicted orthologues in T. brucei with their gene ID as they are found on tritrypdb.org

Protein name used in thesis	*T. brucei* homolog Gene ID.	*S. cerevisiae* homolog	Human homolog
TbCfd1	Tb927.7.1500	Cfd1	CFD1
TbCia1	Tb927.8.3860	Cia1	CIAO1
---	absent?	Absent	FAM96A
TbCia2A*	Tb927.9.10360	Cia2	FAM96B
TbCia2B*	Tb927.8.720		
TbDre2	Tb927.8.1750	Dre2	CIAPIN1
TbMms19**	Tb927.8.3920 Tb927.8.3930	Met18	MMS19
TbNar1	Tb927.10.10650	Nar1	IOP1
TbNbp35	Tb927.10.1690	Nbp35	NBP35
TbTah18	Tb927.4.1950	Tah18	NDOR1

* *H. sapiens* and *T. brucei* have two orthologues of the yeast Cia2 protein, but both of them are more similar to FAM96B than to FAM96A. Trypanosoma Cia2 was named after the yeast Cia2 homolog, and as there are two orthologues they were named Cia2A and Cia2B. TbCia2B was chosen to be B as it has slightly higher similarity to FAM96B than TbCia2A.

***T. brucei* has two nearly identical copies of Mms19

Table of contents

1 Introduction

1.1 *Trypanosoma brucei*

Trypanosoma brucei is a parasitic protozoan belonging to the class of kinetoplastida. Subspecies of *T. brucei* are the causing agents for diseases like sleeping sickness or nagana. This lead to the establishment of *T. brucei* as a model organism in molecular biology. As such it became a valuable tool to study not only its pathogenic properties but also many other traits. *T. brucei* is a representative of the super-group excavate and is considered to belong as kinetoplastida to one of the earliest branching groups in the eukaryotic phylogenetic tree [1][2]. It possesses only one mitochondrion which makes it a good model to study mitochondrial processes. Additionally *T. brucei* undergoes different life stages throughout its parasitic life of which two are regularly used as model stages in laboratory conditions: the bloodstream form which it is present while parasitizing the vertebrate host; and the procyclic form, prevalent in the midgut of the insect vector. While the bloodstream form depends on glycolysis of blood sugars as its main carbon and energy source and has a reduced mitochondria, the procyclic stage has a fully functional mitochondria and obtains energy by oxidative phosphorylation using proline as carbon source, but are also able to grow on glucose rich media under laboratory conditions [3].

Available molecular biology tools like RNA interference (RNAi) and the possibility to knock out, mutate or tag genes together with its fast generation time and a fully sequenced genome, makes *Trypanosoma brucei* a valuable model organism leading to many outstanding discoveries like for example RNA editing [4].

1.2 Iron-sulfur cluster and Iron Sulfur Cluster Proteins

Iron-sulfur (Fe-S) clusters are inorganic prospective groups, usually associated with functionally conserved proteins. They are present in all domains of life and are involved in fundamental biological processes like DNA replication, nucleotide metabolism or electron transport in respiratory or photosynthesis complexes [5]. Despite their function in essential processes there is also one recently reported case where *E. coli* is able to survive without detectable clusters in any of its proteins [6].

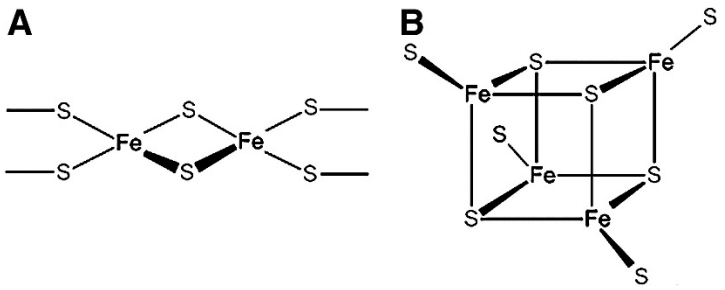

Figure 1: Basic structure of the most common Fe-S clusters, (A) the rhombic [2Fe-2S] and (B) the cubic [4Fe-4S] [7]

The most frequently observed Fe-S clusters bound to proteins are the rhombic [2Fe-2S] cluster (Figure 1A), the cubic [4Fe-4S] cluster (Figure 1B) or the [3Fe-4S] cluster formed by interconversion between [4Fe-4S] and [3Fe-4S] through loss of one iron [8]. Also higher nuclear clusters are found like the [8Fe-7S] as well as co-clusters in which some iron atoms are replaced by other metals as in [7Fe-9S-Mo] which can be found in some nitrogenases of bacteria [9].

The high conservation of many Fe-S cluster proteins present in all living organism suggests a very early evolution of Fe-S clusters and their incorporation into proteins [7], leading even to the theory of Fe-S cluster being responsible for the emerging of life fitting to the iron and sulfur rich environment of the early earth [10]. This theory, however, was later revised, but still Fe-S cluster are given credit to be involved in the evolution of the RNA world, and for being important redox factors for the generation of early organic compounds [11].

The positioning of the iron between the sulfur atoms in the Fe-S cluster allows it to delocalize its electron throughout the cluster, allowing the iron to easily switch its oxidation state between +2 and +3, which accounts for the frequent involvement of Fe-S clusters in electron transport [8]. *In vitro* the clusters may undergo transitions at redox potentials ranging from -700 mV to +400 mV, and with fine-tuning of the protein environment most of this range can be exploited in nature [12]. This allows the clusters to act as excellent electron acceptors as well as donors, and they can be found in many catalytic centers of redox enzymes such as ferredoxins, hydrogenases or respiratory complexes I-III [13]. Other functions involve catalytic activities in enzyme reactions, for example in aconitase, where the cluster helps to coordinate one of the carbonyl groups of citric acid to assists in the elimination of water [14]. In some cases the exact function of the cluster is unknown, where they have been hypothesized to perform a purely structural role, as may be the case of ATP-dependent helicases [13].

Despite their versatile and conserved properties, and their essential role in many fundamental processes in nature, Fe-S clusters remained undetected till in the year 1960 when Electron Paramagnetic Resonance (EPR) spectroscopy allowed the detection of a non-haem based iron containing cofactor [15]. Later it was shown by isotope substitution experiments of iron that the EPR signal of this non-haem cofactors were made up by a significant amount by a signal coming from sulfur [16]. While research was focused initially only on a few proteins, many more have been found belonging to these group of iron-sulfur (or iron-sulfur cluster) proteins [7].

The majority of Fe-S clusters in proteins are ligated by formation of thiolates coming from cysteine residues, apart from a few others like histidine, and in rare cases, glutamine or arginine. Serine is quite similar in its structure as cysteine and was therefore frequently use for the generation of modified Fe-S proteins [17]; there is however no proper documented case in which serine acts as natural ligand. *In-silico* prediction of Fe-S proteins and binding places for Fe-S clusters encounters difficulties, as there seems to be only two conserved binding motives: the $CX_4CX_2CX_{30}C$ motif for the [2Fe-2S] cluster, in plants and mammalian ferredoxins, and the $CX_2CX_2CX_{20\text{-}40}C$ motif for [4Fe-4S]-ferredoxins which can also be found in other [4Fe-4S]-cluster proteins [18]. Usually Fe-S cluster binding cysteine motifs are flanked by a conserved proline or glycine residues, which are needed to stabilize the required spatial arrangement of the cysteines [18]. But apart from these two motifs there are other proteins which do not follow these Fe-S cluster binding patterns, and there are also similar looking cysteine motifs which bind other metals and not clusters [18]. From the identified 3D structures of Fe-S proteins around 50 different folds, mostly for the low potential [2Fe-2S] and few [4Fe-4S]-clusters, have been identified and are believed to represent the majority of all folds [17]. This could help identify new Fe-S proteins from the primary sequence, and help to discern the function of Fe-S proteins with unknown function.

1.2.1 Iron Sulfur Cluster assembly pathways

Iron-sulfur clusters are often labile and susceptible to oxidation, easily leading to the loss of clusters of extracted proteins *in vitro*. Additionally, eukaryotic Fe-S proteins recombinantly expressed in bacteria frequently possess no cluster and they have to be loaded with clusters *in vitro* after purification [19]. Already in the very early stages of the investigation of Fe-S proteins (around 1960) scientists were trying to reconstitute ferredoxins, which was achieved by addition of reducing agents, free iron and sulfides *in vitro* [20]. Further research showed that maturation of Fe-S proteins *in vivo* is a rather

complex process required protein-driven catalytic steps [5][21]. Reconstitution of Fe-S proteins into apoproteins *in vitro* implies the use of conditions outside the concentrations of cellular physiological range, together with the instability of the Fe-S cluster free in solution. A coordinated process is therefore required to assemble the cluster, while protecting the cell from high free iron and sulfide concentrations, while also protecting the newly assembled cluster form the surrounding solution [7].

Currently three machineries for Fe-S cluster assembly have been identified in bacteria: the nitrogen fixation (NIF) system, which is required for the certain nitrogenases in azototrophic bacteria (bacteria which fix their own nitrogen); the iron-sulfur cluster (ISC) system, which is required for the maturation of Fe-S proteins under normal conditions; and the sulfur utilization factor (SUF) system which is active under oxidative stress conditions [22]. Over the endosymbiotic event in which eukaryotes acquired mitochondria they also took over proteins of the ISC machinery (and some SUF proteins), so that the ISC machinery is present in all mitochondria containing eukaryotes [23], while the SUF machinery got transferred together with plastids and is therefore encountered in all plastid containing eukaryotes [24]. Additionally eukaryotes obtain a third Fe-S cluster assembly machinery, which is however dependent on the ISC machinery, called the cytosolic iron sulfur cluster assembly (CIA) machinery, required for the maturation of [4Fe-4S] cluster proteins in cytosol and mitochondrion [25][26].

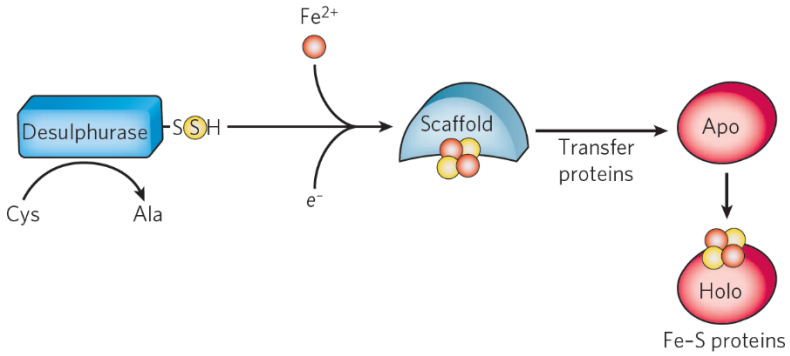

Figure 2: Basic steps of Fe-S cluster assembly and Fe-S protein maturation [13]

Each of the biosynthesis pathways may be split into two general parts (see Figure 2). First, the cluster must be assembled, and in the second step it is transferred onto the apoproteins. For the initial step a cysteine desulfurase has to release sulfur from a cysteine, and generate a persulfate intermediate. The iron, usually very low as free molecule in the cell, is delivered by specific iron donors. The sulfur (S^0) in cysteine is reduced to sulfide (S^{2-}) by an electron donor. The cluster is further assembled on a scaffold protein, which provides

a binding pocket for clusters made from conserved cysteines. The cluster binds weakly to the scaffold, for its further transfer into the apoprotein. This step may be either protein-assisted *in vivo* or directly from the scaffold to the immature Fe-S protein *in vitro* [13].

The first identified Fe-S cluster assembly pathway in bacteria was the NIF system in *A. vinelandii*, required solely for the maturation of nitrogenases [27]. Upon deletion of the NifS gene a homologue termed the IscS was identified. Together with the sequence of the IscS gene and the NifS operon, the *isc* operon was identified, comprising the genes IscS, IscU, IscA, IscB, hscA, and fdx [28]. Homologues of these genes have been identified in other prokaryotes [29] as well as in eukaryotes, such as plants [30], yeast [29] and humans [31]. As one of the eukaryotes the ISC assembly pathway was also found to be conserved in *T. brucei* [32]. Fe-S cluster maturation was also found to be conserved to the mitosomes in *Giardi intestinalis* which led to the suggestion that the main essential function of mitochondria is the maturation of Fe-S cluster proteins and not the obvious production of ATP and energy [33].

Eukaryotic ISC was first and has been best studied in yeast, and findings from yeast have served to find orthologues in other eukaryotes. Therefore here I will focus on the function and mechanism of ISC from *S. cerevisiae* using the nomenclature for yeast as shown in Figure 3. This figure should also help as a general guide for the understanding of the ISC and CIA machinery as described from here on.

The basic ISC starts with the assembly of a [2Fe-2S]-cluster on the scaffold protein Isu1 (homologue of bacterial IscU) which possesses a binding pocket for the newly formed cluster [34]. The assembly on Isu1 requires the cysteine desulfurase complex comprised of the proteins Nfs1 (related to bacterial NifS) and Isd11, which reduces a free cysteine to alanine forming a per-sulfide intermediate on Nfs1 [35][36]. The required iron is imported into the mitochondria over the carrier complex Mrs3-Mrs4 and further delivered to the Nfs1-Isd11-Isu1 complex [37]. This transport to Isu1 is facilitated by frataxin (Yfh1). The exact mechanism and function of frataxin in this process remains unknown [38][39]. For the reduction of the sulfur from cysteine to form per-sulfide, reduction of NAD(P)H by ferredoxin reductase (Arh1) is required. Further electron transfer is performed by Isu1 and ferredoxin (Yah1) [40]. After assembly, the cluster is ready to be released from the scaffold via the Fe-S cluster transfer protein Grx5 and transported to its target proteins. This step is further aided by the Hsp70 chaperon system, which includes the Hsp70 ATPase Ssq1,

co-chaperon Jac1, and the nucleotide exchange factor Mge1, which after release also helps the transfer of the cluster from Isu1 on the transfer protein Grx5 [41].

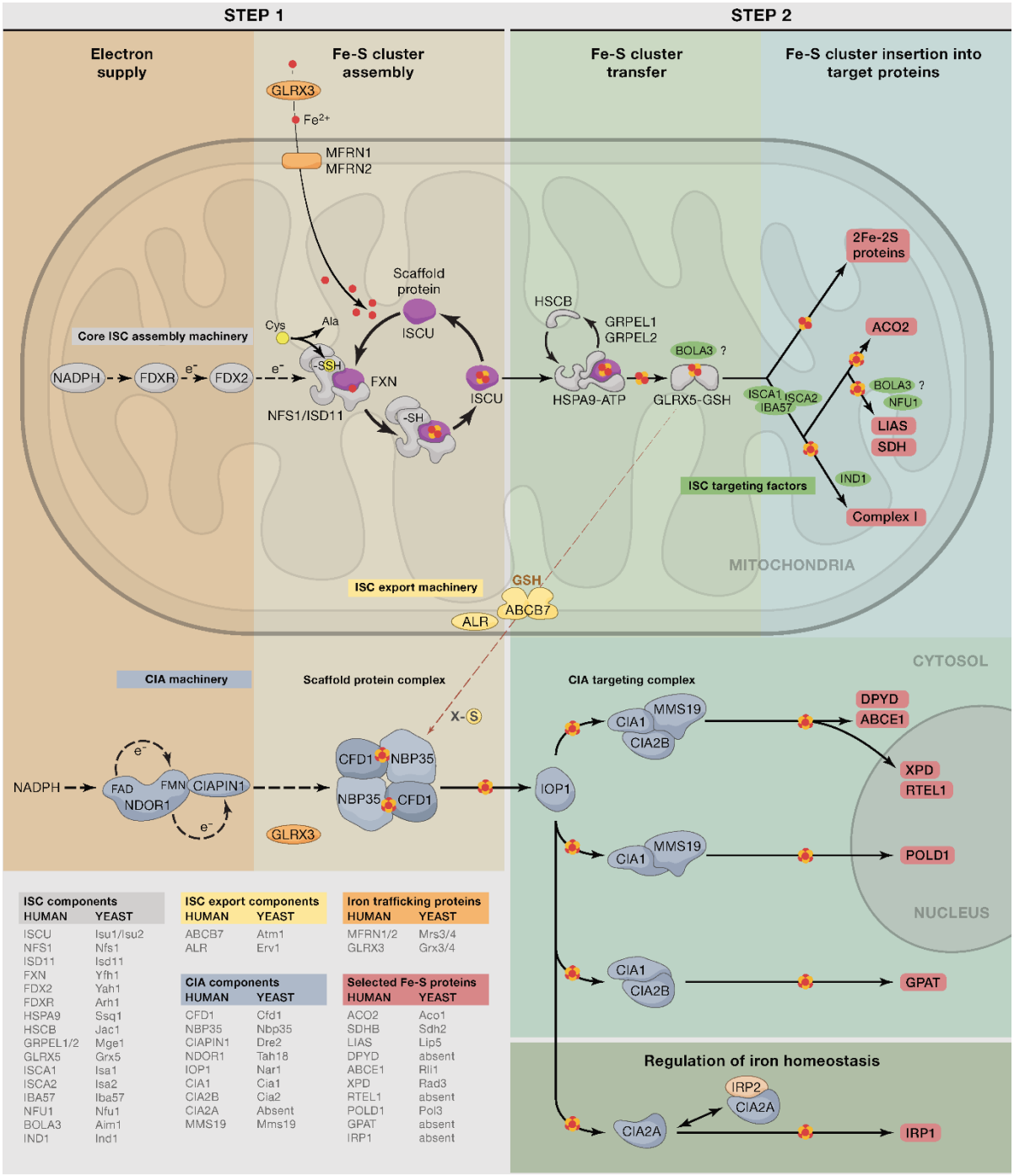

Figure 3: Overview of the Fe-S biogenesis pathways in eukaryotes, ISC in mitochondria and CIA in cytosol [42]

Downstream of Grx5 three targeting factors, the ISC targeting factors Isa1, Isa2 and Iba57, form a complex required to insert the [2Fe-2S] cluster into the mitochondrial Fe-S apoproteins [43]. These factors are also required for the formation and insertion of [4Fe-4S] clusters in mitochondria [44], but the mechanism how they generate the [4Fe-4S] cluster from the [2Fe-2S] cluster is unclear [45].

1.2.2 Cytosolic Iron Sulfur Cluster Assembly (CIA)

The cytosolic iron sulfur cluster assembly presumably developed partially independent from the Fe-S cluster assembly systems known from bacteria as it had to arise in response to the development of compartments in eukaryotes [7]. Cluster assembly systems from bacteria seem to have evolved to function localized restricted to the compartments from endosymbiosis, such as mitochondria and chloroplasts. Moreover, the lack of transport systems for the assembled clusters demands an independent configuration of Fe-S cluster assembly in the cytosol, namely the CIA system [26]. Nevertheless the CIA pathway is not a completely independent Fe-S cluster assembly system, as it requires a sulfur-containing compound which originates from the mitochondrial ISC system, therefore linking both pathways [46]. Also the CIA machinery is not maturating all Fe-S proteins in the cytosol, but so far it has been the only fully functional Fe-S cluster assembly machinery characterized in the cytosol [47]. So far, eight core components of the CIA pathway have been identified: Cfd1, Nbp35, Tah18, Dre2, Nar1, Cia1, Mms19 and Cia2, most of them essential for yeast viability [26]. These eight components are highly conserved and phylogenetic analysis showed that they were probably already present in the last eukaryotic common ancestor (LECA) [48].

As the other cluster assembly systems, the CIA may be divided into two main processes: cluster assembly and cluster transfer. The assembly begins with *de novo* synthesis of the cluster on a scaffold comprised of a heterotetramer formed by two subunits of the nucleotide binding protein 35 (Nbp35) and another two of the cytosolic Fe-S cluster deficient 1 protein (Cfd1) [49]. Both Nbp35 and Cfd1 are homologues proteins, which fall into the superfamily of the P-loop NTPases. While both proteins are essential in yeast, only Nbp35 is present in the genome of *Arabidopsis* and a homodimer of Nbp35 acts as scaffold for the cluster assembly [50]. It has to be pointed out that the Cfd1-Nbp35 scaffold facilitates an assembly of a [4Fe-4S] cluster, and in general the CIA system involves assembly and maturation of [4Fe-4S] cluster proteins. It is unknown if the CIA is also capable of assembling [2Fe-2S] clusters or if there is an additional assembly pathway special for [2Fe-2S] cluster proteins in the cytosol [25]. Both Cfd1 and Nbp35 contain a nucleotide binding domain, characteristic for P-loop NTPases and four conserved cysteine residues in their C-terminus. The two central cysteine residues bind a bridging [4Fe-4S] cluster, required for the formation of the heterotetramer, while the other two cysteines seem to be expendable

despite their high conservation. However the nucleotide binding domain appears to be essential for the cluster assembly, indicating that this step is a energy-requiring step [51][52].

The assembly of the cluster requires three components as described before for the ISC system, a source of iron and, sulfur and electron donor molecules for the reduction of the sulfur to sulfide. The sulfur compound is donated via the ABC transporter Atm1, described as part of the mitochondrial ISC export machinery. Atm1 exports a glutathione-containing compound out of the mitochondria. The sulfhydryl oxidase Erv1, involved in the import of sulfur containing molecules in the mitochondria, was initially included as a component of the ISC export machinery [53]. This initial affirmation was made on data from knockdowns of Erv1 in yeast displaying similar phenotypes to those for Atm1 [54]. However, a recent study showed that Erv1 is not linked to any form of modulation of the cytosolic Fe-S cluster assembly, and the observed phenotype most likely results as a secondary effect from the impaired maturation of glutathione upon downregulation of Erv1 [55].

The electrons for the cluster assembly are provided by an electron transport from NADPH over Tah18 to Dre2 and further passed to the Cfd1-Nbp35 scaffold. The diflavin oxidoreductase Tah18 contains a FAD and a FMN binding domain, binds a NADPH and physically interacts with Dre2 [56]. Dre2 possesses a N-terminal S-adenosylmethionine (SAM) methyltransferase-like domain which does not show binding to SAM, as it lacks part of the SAM binding pocket, but it still contains the full substrate binding motif [57]. On its C-terminus it contains two conserved cluster binding domains, each comprised of four conserved cysteines, which bind one [2Fe-2S] and one [4Fe-4S] cluster [58]. Electrons from the oxidation of NADPH are passed to the FAD group of Tah18 and further transferred to FMN, to be received by the [2Fe-2S] cluster of Dre2 [59]. However, the precise site of charge delivery on the scaffold is unknown. Also this electron transport module is only required for the maturation of CIA target proteins and not for the assembly of the bridging [4Fe-4S] cluster contained in the scaffold protein complex Cfd1-Nbp35 [47].

The source for iron for the assembly in cytosol is unclear; however, it has been proposed that the cytosolic monothiol glutaredoxins Grx3 and Grx4 are required for this process in yeast. Depletion of Grx3/4 in yeast cells produces defects in iron insertion into proteins indicating their involvement in the CIA pathway. Their exact function and mechanism of action in the CIA pathway however, has not been clarified [60].

The assembled clusters are transferred to the CIA targeting complex by the transfer protein Nar1. The iron-only hydrogenase-like protein Nar1 is essential for yeast viability and for Fe-S protein maturation in the cytosol [61][62]; it has also been shown to physically interact with Nbp35, to bind the newly assembled cluster and transport it further [49]. It also binds transiently to the CIA targeting proteins, indicating that it has the bridging role between the targeting machinery and the cluster assembly on the Cfd1-Nbp35 scaffold [63][64].

1.2.3 CIA targeting complex

The CIA targeting complex has the function to transfer the newly assembled clusters onto the cytosolic Fe-S cluster apoproteins. In human, the targeting machinery involves five proteins, CIA1, MMS19, CIA2A, CIA2B and ANT2 [65][66]. In yeast, this complex is comprised of only three components: Cia1, Met18 and Cia2 [67].

The cytosolic iron-sulfur protein assembly 1 protein (Cia1) is a WD40 repeat protein. WD40 repeat proteins frequently function as coordinators of multi-protein complexes. They possess seven repeating β-sheet units, which serve as protein binding stations, allowing them to perform a scaffolding function. In yeast, Cia1 is dually localized in both cytosol and nucleus, whereas the nuclear content makes up for the majority of Cia1 present in the cell. While function of Cia1 in the nucleus is unknown, it binds to Nar1 in the cytosol [64]. Studies in human showed that CIA1 also binds tightly to CIA2B (orthologue of yeast Cia2), and CIA2B binds MMS19, linking these two proteins [63][68]. In humans, depletion of one of the components also leads to down regulation in expression of its counterparts, while in yeast, both Mms19 and Cia2 seem to directly bind to Cia1, as down regulation of Cia1 leads to decreased association of Cia2 with Mms19 [69].

MMS19 has been known for long to be connected with DNA repair and transcription, but the mechanism of its involvement in this processes remains unknown [70]. The size of Mms19 and the presence of HEAT repeats, domains containing chains of specific nearly identical folds, frequently encountered for binding of proteins, initially suggested that it may be the scaffold of the CIA targeting complex [71]. Previous experiments showed that it interacts directly with XPB and XPD, helicase subunits of the transcription factor TFIIH, a complex working in nuclear excision repair (NER) pathway [72], only to be identified later as member of the CIA pathway functioning in the Cia1-Mms19-Cia2 complex for targeting of Fe-S clusters [73].

In the last few years a series of pull-down experiments in humans, yeast and plants, have been performed on CIA1, MMS19, CIA2A, and CIA2B, which gave insight into the complexity of the CIA targeting machinery, its components and targets [63][65][66][73][74][75]. Additionally selected targets were also investigated using specific enzyme assays to further investigate their function [66]. The experiments revealed that various sub-complexes are targeting defined seta of Fe-S apoproteins (Figure 4). Each of the complexes has CIA1 as central mediator, as it can interact with IOP1 (yeast Nar1), which transfers the [4Fe-4S] cluster received from the CFD1-NBP35 assembly complex. The three main conserved late acting CIA components CIA1, MMS19 and CIA2B form 2 binary complexes, CIA1-CIA2B and CIA1-MMS19, and one ternary complex containing all three components, CIA1-MMS19-CIA2B as depicted in Figure 4 [26].

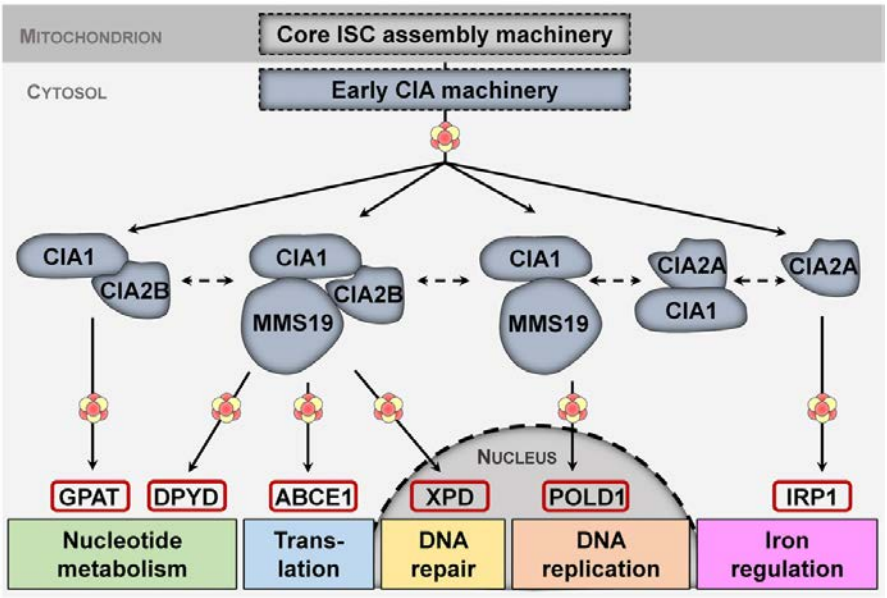

Figure 4: Different sub-complexes of the late acting CIA components target specific subsets of nuclear and cytosolic Fe-S proteins, while the complexes themselves interconvert dynamically [26]

The CIA1-CIA2B complex interacts specifically with the glutamine phosphoribosyl-pyrophosphate amidotransferase (GPAT), which contributes to nucleotide metabolism. CIA1-CIA2B-MMS19 forms the largest complex, targeting the majority of all Fe-S cluster proteins in cytosol and nucleus. It was shown to interact with the dihydropyrimidine dehydrogenase DPYD and ABCE1 which further interacts with translation initiation factors, in cytosol and nuclear with XPD, a helicase subunit of the TFIIH complex and RTEL1, the regulator of telomere elongation helicase 1. A distinct subset of proteins does not require CIA2B, and their maturation depends on the CIA1-MMS19 complex. One of these proteins is the DNA polymerase catalytic subunit alpha POLA1 [66][67]. DNA polymerase catalytic subunit delta 1 POLD1 was shown to interact with CIA1, MMS19 and CIA2B, but RNAi

knockdown studies of CIA2B showed that it is dispensable for the maturation of POLD1. Similar MMS19 interacts with GPAT but is not necessarily required for its maturation [66]. These two observations suggest that the CIA targeting complex is dynamic and might not need to be strictly assembled to perform the function of the individual sub-complexes.

CIA1 forms mutual exclusive complexes with either CIA2A or CIA2B, but no experiment showed a simultaneous interaction with both CIA2 homologues. CIA2A takes a special role in the CIA pathway, as it is present in human, where it was shown to interact with the iron regulatory protein 2 (IRP2), but is absent in yeast. Knockdown of CIA2A down regulates the expression of the IRP2 and reduces the activity of cytosolic aconitase, the holo-form of IRP1, but the physical interaction found between CIA2A and IRP1 has not been found. Additionally, depletion of CIA1 shows no effect on iron metabolism, which questions the role of the CIA1-CIA2A complex [66].

ANT2 was often co-purified and detected in mass spectrometry as high abundant interaction partner of CIA1, CIA2B and MMS19. Detailed investigations showed that it does not interact directly with CIA1 or CIA2B, but it helps to stabilize the binding of target Fe-S proteins to MMS19 by bridging MMS19 with the target protein. It was found only present when the target proteins binds to MMS19 and is not a permanent part of the CIA1-MMS19-CIA2B complex [65].

Many Fe-S proteins were identified using pull-down experiments and they were shown to interact with one of the CIA targeting complexes, suggesting that they are substrates of the CIA pathway; this however still must to be validated by suitable biochemical experiments. Also the mechanism of the cluster transfer is still unknown. CIA1 functions as scaffold to bind MMS19 and CIA2B, and links to IOP1, but MMS19 and CIA2B have just protein-binding functions but no domains to transiently bind Fe-S clusters. So the main function of the CIA targeting complex is to bring the Fe-S protein targets close together to IOP1. However, if the cluster is directly transferred from IOP1 to the apoproteins or if additional factors are required for the transfer, remains to be investigated.

1.2.4 CIA in *Trypanosoma brucei*

Little is known about the cytosolic iron sulfur cluster assembly in species of the eukaryotic super group Excavata. In Trypanosomatids all eight CIA components are genetically conserved [1][48] as well as the ISC export machinery's Atm1 [1]. The current model for the CIA in *T. brucei* is summarized in Figure 5.

TbAtm silencing showed a mild growth defect and a decrease on cytosolic aconitase activity identifying it as part of the ISC export machinery [76].

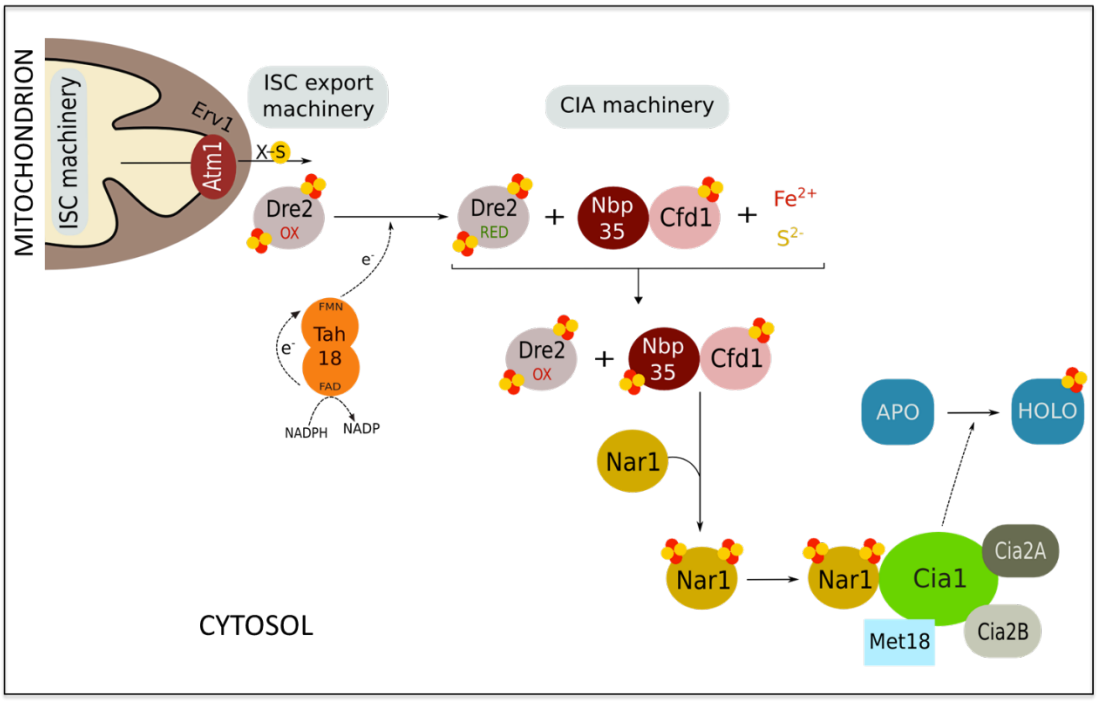

Figure 5: CIA machinery in T. brucei

Knock-down of TbCfd1 or TbNbp35 shows a strong growth phenotype and an accumulation of non-thiolated tRNAs in the cytosol [77]. Both of them contain four c-terminal conserved cysteine residues for bonding of a bridging [4Fe-4S] cluster, and TbNbp35 contains a second set of four cysteine residues near its N-terminus required for the assembly of the new cluster. Knockdown of TbNbp35 or TbCfd1 also shows a decrease in cytosolic aconitase activity [78].

TbTah18 is a diflavin oxidoreductase that transfers electrons from NAD(P)H to TbDre2. TbDre2 lacks the N-terminal SAM methyltransferase domain, which is conserved in human and yeast Dre2, but it retained the conserved cysteine residues and was shown to bind a [2Fe-2S] cluster. The individual RNAi knockdowns showed no growth phenotype, and only TbTah18 RNAi showed slight decrease in aconitase activity. A double knockdown of TbTah18 and TbDre2, exhibited a growth phenotype and a nearly complete abolishment of c-aconitase activity, confirming the interaction of TbTah18 with TbDre2 in their possible role of electron provider for the CIA machinery. A complementation assay in yeast additionally showed that an expression of TbTah18 together with TbDre2 in a yeast strain ablated of the yeast orthologous, was able to completely rescue growth. This result confirms that the *T. brucei* CIA genes perform similar function as their homologues in yeast [78].

A further double knockdown of TbDre2 and TbNbp35 lead to a stronger decrease in c-aconitase as well as an even stronger growth phenotype than the single knockdown of TbNbp35 alone, affirming the interplay of TbDre2 with TbNbp35 for transfer of the electron required for the cluster assembly [78].

Downregulation of the cluster transporter TbNar1 showed slight effect on c-aconitase activity, and knockdown of the target complex scaffold TbCia1 only showed moderate decrease. Individual RNAi performed on each of these components showed no growth defect neither in procyclic nor in bloodstream forms *T. brucei*. On the other hand, the double knock down of TbCia1+TbNar1 displayed a strong impairment in growth in both life stages and lead to a complete loss of c-aconitase activity, linking these two components as key players for the maturation of c-aconitase, and in general Fe-S cluster protein maturation in cytosol [78].

The further components of the CIA targeting machinery are Mms19 and Cia2. *T. brucei* has two nearly identical copies of the TbMms19 gene resulting in proteins with ~99% amino acid identity. RNAi silencing targeted against both copies of TbMms19 shows no effect on growth and no influence on c-aconitase activity.

T. brucei also contains two copies of Cia2, called TbCia2A and TbCia2B, which share approximately 36% amino acid identity. TbCia2B shows a closer resemblance to FAM96B and yeast Cia2, than does TbCia2A. It also was shown that TbCia2B, but not TbCia2A, was able to functionally complement a ΔCia2 yeast mutant. Neither TbCia2A nor TbCia2B show an effect on growth of *T. brucei* when silenced by RNAi, and they also exhibit no observable effect on c-aconitase activity [unpublished results].

2 Aims of the thesis

The aim of this thesis was to determine the localization and find out interaction partners of the late acting components of the cytosolic iron-sulfur cluster assembly pathway. As there are no are no antibodies for this proteins available which are specific enough to use them for localization through immunofluorescence assay or co-immunoprecipitation, the proteins had to be tagged with a non-interfering tag which then can be targeted with a specific antibody and be used for fluorescence microscopy and for a pull-down experiment. The pull-down should be analyzed by mass spectrometry to find the possible substrates and interaction partners of the proteins of interest. As supporting experiment the influence of the knock-down of the late CIA components on the cytosolic aconitase should be studied by activity assays.

3 Materials and Methods

3.1 Cultivation of *Trypanosoma brucei*

29-13 [79] and SmOxP9 [80] were used as parental cell lines of procyclic *Trypanosoma brucei*. Cells were cultivated in SDM-79 medium supplemented with 10% fetal bovine serum at 27°C [81] and 2.5 µg/mL hemin. The 29-13 cell line was grown under the presence of hygromycin (50 µg/mL) and G418 (15 µg/mL) [79]. Knock-down cell lines were additionally supplemented with phleomycin (2.5 µg/mL) and tetracycline (1 µg/mL) for induction of the RNAi. The cell line SmOxP9 was grown under the presence of the puromycin (1 µg/mL) and SmOxP9 v5-tagged cell lines with hygromycin (50 µg/mL) for c-terminal tagged proteins [82].

RNAi cell lines of TbCia2A (TbCia2A-RNAi) and TbCia2B (TbCia2B-RNAi) were constructed by Somsuvro Basu and the double knockdown cell lines against TbCia1+TbCia2B (TbCia1+TbCia2B-RNAi) and TbCia2A+TbCia2B (TbCia2A+TbCia2B-RNAi) constructed by myself during the work on my bachelor thesis.

3.2 Preparation of v5-tagged cell lines

Primers were designed according to the protocol for endogenous C-terminal tagging using the pPOTv4 plasmid. Primers for TbCia1, TbMms19 and TbCia2A were designed by Sam Dean using the tagit perl script [82], the primer for TbCia2B was designed manually. A summary of the used primers is given in Table 2.

Table 2: Primers for generation of C-terminal tagged proteins using the pPOTv4 vector, FP…forward primer, RP…reverse Primer

Name	5'-3' Sequence
TbCia1 C FP	GTCGAGGTGG CGAAGGTTTG TTGTTAGCGT CGGGCGGTGA TGATAATATC GTACGTATTT GGCGCGTGAC TGCAGCGCTG ggttctggtagtggttcc
TbCia1 C RP	GTAGATATTA AAAGCTAAAG AAAATTGGGC GCCGATTTAA CACCTGCGCA CTGCCGATCC CAGACACACA CCCTCTCTCT ccaatttgagagacctgtgc
TbMms19 C FP	CTCAGGTGGC ATTGAGTGAT CACAAGCGGA TGGTGCGACG TAGTGCCGCT CAGTGCCGGC ATCAGTGGTA TAAATTAAAG ggttctggtagtggttcc
TbMms19 C RP	CAGGCGGCGC CTCCTCCTCT TCATGTGCGG GAAACAAAAC TGAGAAAACA AAACTTACAC GGTTTATATG GCTTACGCAA ccaatttgagagacctgtgc
TbCia2A FP	TTGCAGACAA GGAGAGACTG GCGGCAGCAA TGGAGGACAA GGCGCTTCTA CAGGAAGTTG AGAGGCATAT TAATTGTGAG ggttctggtagtggttcc
TbCia2A RP	TTCTACTTTC CACAGTTCCA CCGAAGGCGT GGAACGGCAT ATGTGCTAAT ACGAATGAAG GGAAGGAGGA AGAGAAGAGT ccaatttgagagacctgtgc
TbCia2B FP	GCGACAAGGA ACGTGTGGCT GCTGCGTTAG AAAACACAAA CCTCTTAAAT GTAGTGGAAT CATGCGTAAA TGCCTTTGAA ggttctggtagtggttcc
TbCia2B RP	ACTCCCTCTT ACGTCGTTGT TTTATTTATT TTTTTTAAAA AAGGGGGGGG CACAAAAAAA AAAAAAGAGG AATTAAACAC ccaatttgagagacctgtgc

A modified pPOTv4 plasmid in which the eYFP tag was replaced by 3xV5, termed pPOTv4-v5. The plasmid was constructed by Michala Boudová including a stop codon at the end of the v5-tag.

DNA was amplified by "hotstart" PCR according to the published protocol [82] and was used without further purification directly for the electroporation. For the "hotstart" PCR, mixture A (Table 3) was placed into the thermocycler and the PCR program (Table 5) was started. After the machine reached 94°C for 1 min, mixture B (Table 4) was added. The hotstart ensures less unspecific amplifications due to unspecific binding of the primers to the template before the first cycle where the polymerase already could be active.

Table 3: PCR Mix A

Mix A	Volume
DMSO (PCR grade)	0.5 µL
Forward Primer, 100 µM (final conc. 2 µM)	1 µL
Forward Primer, 100 µM (final conc. 2 µM)	1 µL
25 ng Template (pPOTv4-v5, 25 ng/ µL stock)	1 µL
dNTPs, 10 mM each (final conc. 0.2 mM)	1 µL
MiliQ	44 µL
Total	50 µL

Table 4: PCR Mix B

Mix B	**Volume**
Expand HiFi buffer 2 (Roche, 04 743 725 001)	5 µL
Expand HiFi polymerase (Roche, 04 743 725 001)	1 µL
MiliQ	19 µL
Total	25 µL

Table 5: PCR program

Temperature	**Time**	
94°C	5 min	
94°C	15 sec	
50°C	30 sec	
72°C	2 min	2↑ 30 cycles
72°C	2 min	
16°C	pause	

After completion of the PCR cycle, 5 µL of the reaction mixture was loaded on a 0.75% agarose gel, 0.1 µg/mL Ethidium bromide, and ran at 100V for 30 min. DNA was visualized under UV light.

For the each electroporation $1x10^7$ cells of a mid-log SmOxP9 culture were spun down at 800 x *g*, at room temperature (RT) for 10 min. The cell pellet was resuspended in 400 µL Cytomix (25 mM HEPES, 120 mM KCl, 0.15 mM $CaCl_2$, 10 mM K_2HPO_4/KH_2PO_4, 2 mM EDTA, 6 mM Glucose, 5 mM $MgCl_2$, pH 7.6), mixed with 45 µL PCR reaction mixture, and electroporated (1600 V, 25 Ω and 50 µF) in a 0.2 cm gap electroporation cuvette on a BTX ECM650 Electro Cell Manipulator®. One electroporation was performed without adding any PCR mixture to serve as negative control. Cell suspension was immediately mixed with 9.5 mL fresh SDM-79 containing puromycin (1 µg/mL) and allowed to recover overnight (8-16h, 27°C). 20 mL of fresh media with puromycin (1 µg/mL) and hygromycin (100 µg/mL) were added to the culture for selection and the culture was plated completely in a 24-well plate. After 10-14 days and no living cells in the negative controls could be observed, wells were screened for live cultures, which were subsequently screened for expression of the v5-tagged protein. One positive clone for each cell line was selected and grown to higher volume for further experiments, and an aliquot was also prepared for long time storage in liquid nitrogen.

3.3 Immunofluorescence assay (IFA)

For localization studies the v5-tagged cells were analyzed by an immunofluorescence assay (IFA). Cells were grown to densities between 0.5-1x10^7 cells/mL. 1 mL of the cell suspensions was spun down at 1000 x *g* and RT for 2 min on a tabletop centrifuge. For visualization of mitochondria, cells were incubated 27°C for 30 min with 200 nM MitoTracker® Red CMXRos (ThermoFisher scientific). Cell pellets were resuspended in 1 mL of 4% (w/v) paraformaldehyde in PBS (phosphate buffered saline: 137 mM NaCl, 2.7 mM KCl, 4.3 mM Na_2HPO_4, 1.47 mM KH_2PO_4, pH 7.4), and 1.25 mM NaOH for 10 min to fix the cells. Cells were centrifuged at 1000 x *g* for 2 min and all except 100 µL of the supernatant was removed. The cells were resuspended in the remaining 100 µL and spread on Superfrost® plus slides (Thermo scientific) and left to settle for 30 min in a humid chamber. The formaldehyde was pipetted off and the slide was washed short in PBS. The cells were permeabilized in ice cold methanol for 20 min followed by 0.2% (v/v) TX-100 in PBS for another 20 min. After permeabilization of the cells, the slides were washed once for 5 min in PBS and then incubated for 2 h at RT with the primary antibody dissolved in milk (5% (w/v) milk powder in PBS-T (PBS with 0.05% (v/v) Tween20)).

Cells incubated with MitoTracker® Red were immunodecorated with monoclonal α-v5 mouse antibody (ThermoFisher scientific, 37-7500) at a dilution of 1:1000 in PBS-milk. Cells without MitoTracker®, a monoclonal α-v5 antibody and α -enolase rabbit antibody (provided by Paul Michels, University of Edinburgh) at a dilution of 1:2000 was applied. Enolase was used as a cytosolic marker. For glycosomal staining, polyclonal α-TbHexokinase was used at a dilution of 1:1000 [83], and for nuclear staining α-TbLa antibody was used at a dilution of 1:1000 [84].

The slide was washed 3 times for 5 min in PBS, and incubated for 1 h at RT, with 0.25 mL of secondary antibody dissolved in PBS-milk per slide. For slides containing α-v5 mouse antibody, Goat Anti-Mouse IgG H&L conjugated with Alexa Fluor® 488 (Invitrogen) dissolved at a dilution of 1:1000 in milk was used. For slides containing α-enolase rabbit antibody, Goat Anti-Rabbit IgG H&L conjugated with Alexa Fluor® 555 (Invitrogen) dissolved at a dilution of 1:1000 in milk was used. A summary of the antibodies used may be found in Table 6. The slides were washed 5 times for 5 min with PBS. Slides were mounted with 1 drop ProLong® Gold Antifade reagent with DAPI (molecular probes, P36935) under a coverslip and sealed airtight with nail polish to prevent the sample from drying out. The slides were stored in the dark at 4°C until used.

The samples were observed under the fluorescence microscope or the confocal microscope

for 3D images or images which required sequential recording of the different channels. Image manipulations were performed with Fiji [85].

3.3.1 IFA with NP-40 treatment

For NP-40 treatement, cells were harvested and washed as described in section 3.3. The cells were resuspended in 50 µL NP-40 buffer (10 mM Tris-HCl, pH 6.8, 1 mM $MgCl_2$, 0.25% (v/v) NP-40 (Tergitol® Type NP-40, Sigma-Aldrich)) and spread onto the microscopy slides. After 4 min the buffer was removed and the cells were fixed with 4% (w/v) paraformaldehyde for 10 min. The paraformaldehyde was removed and cells were permeabilized with 100% ice cold methanol for 20 min. The cells were washed once with PBS and blocked for 45 min with 5.5% (w/v) FBS in PBS-T. Cells were washed 2X with PBS and incubated for 2 h with primary anybody diluted in 3% (w/v) BSA in PBS-T (antibodies at dilution 1:1000). Slides were washed 3X with PBS-T and 2X with PBS. Secondary antibody was diluted 1:1000 in 3% (w/v) BSA in PBS-T on slide for 1h. After incubation and washing 3X with PBS-T and 2X with PBS, the slides were mounted with 1 drop ProLong® Gold Antifade reagent with DAPI under a coverslip and sealed airtight with nail polish. Slides were analyzed under a confocal microscope.

Table 6: Used primary and secondary antibodies for IFAs, protein used to use raise the antibody in which organism, dilution used in IFA, cellular localization, source of the antibody. The observed localization for the v5 antibody depends on the tagged protein.

Antibody (target protein)	**Organism**	**Dilution**	**Localization**	**Source**
TbEnolase	Rabbit	1:1000	cytosol	Paul Michels, University of Edinburgh
TbLa	Rabbit	1:1000	nucleus	[84]
TbHexokinase	Rabbit	1:1000	glycosomes	[83]
V5 Epitope Tag	Mouse	1:1000	various	ThermoFisher scientific, 37-7500
Secondary antibodies				
Anti-Mouse IgG peroxidase H&L conjugated with Alexa Fluor® 488		goat	1:1000	Invitrogen
Anti-Rabbit IgG peroxidase H&L conjugated with Alexa Fluor® 555		goat	1:1000	Invitrogen

3.4 Crude cellular fractionation

A modified protocol for the crude fractionation of the cytosol from the organellar fraction in *Trypanosoma brucei* [86] as published in previous studies of this laboratory [32] was used.

Cells were grown in 100 mL to densities between 0.5-1x10^7 cells/mL. 5x10^8 cells were harvested by centrifugation at 1000 x *g*, 4°C for 10 min. The cell pellet was washed twice with ice-cold SHE buffer (25 mM HEPES, pH 7.4, 250 mM sucrose, 1 mM EDTA). The final pellet was resuspended in 100 µL SHE buffer to a concentration of 5x10^9 cells/mL and the protein concentration of the suspension was determined by a Bradford protein Assay. Aliquots corresponding to 1 mg of protein were resuspended in 200 µL of homemade Hanks' balanced salt solution (HBSS) buffer (1.26 mM $CaCl_2$, 5.33 mM KCl, 0.44 mM KH_2PO_4, 0.81 mM $MgSO_4$, 138 mM NaCl, 4 mM $NaHCO_3$, 0.3 mM Na_2HPO_4, 5.6 mM glucose, pH 7.3) and added with an sufficient amount of digitonin (10 mg/mL in MiliQ H_2O) to reach a final concentration of 0.4 µg/µL digitonin. The suspension was vortexed for a few seconds and incubated for 5 min at 25°C (RT). After spinning for 2 min at 14000 x *g* at RT, the supernatant representing the soluble cytosolic fraction was collected and immediately placed on ice for later use; for longer storage it was placed into a -20°C freezer. The pellet obtained from the centrifugation was washed once with HBSS buffer and resuspended in fresh 200 µL HBSS. It was added with Triton X-100 (10% (v/v) TX-100 in MiliQ H_2O) to obtain a final concentration of 0.1% (v/v) TX-100 and incubated for 5 min on ice. The solution was spun as before and the supernatant representing the mitochondrial fraction was collected and placed on ice. The pellet was washed once with HBSS and resuspended in 200 µL HBSS, representing a sample for the insoluble proteins, unreleased membrane bound proteins or other insoluble cell contents. Aliquots of the samples were mixed with 2x SDS-Sample buffer (2xSB, 24 mM Tris-HCL, pH 6.8, 10% (v/v) glycerol, 0.8% (w/v) SDS, 2% (v/v) β-mercaptoethanol, 0.4 mg/mL bromophenol blue) boiled at 98°C for 10 min and analyzed by Western blot.

3.5 Selective permeabilization

For a detailed subcellular fractionation cells were exposed to increasing amounts of digitonin to gradually release the proteins from the different cellular compartments.

To obtain $2x10^8$ cells per examined fraction, $2.2x10^9$ cells of mid-log *Trypanosoma* culture were harvested by centrifugation at 1000 x *g*, 4°C for 10 min, and washed once with PBS. The cell pellet was resuspended in STE-NaCl buffer (25 mM Tris, pH 7.4, 250 mM sucrose, 1 mM EDTA, 150 mM NaCl) using 150 µL buffer per $2x10^8$ cells (final concentration $1.33x10^9$ cells/mL). The cell suspension was divided into 150 µL aliquots, and the aliquots were added up to a final volume of 300 µL with STE-NaCl buffer and STE-NaCl-buffer containing digitonin according to Table 7, to obtain final digitonin concentration reaching from 0 to 1.5 mM.

Table 7: Preparation of digitonin gradient for selective permeabilization

Sample Number	1	2	3	4	5	6	7	8	9	10
Final digitonin concentration [mM]	0	0.05	0.1	0.2	0.3	0.4	0.6	0.8	1.0	1.5
Cell suspension [µL]	150	150	150	150	150	150	150	150	150	150
STE-NaCl buffer [µL]	150	142.5	135	120	105	90	60	30	10	105
STE-NaCl buffer with 2.0 mM digitonin [µL]	0	7.5	15	30	45	60	90	120	140	0
STE-NaCl buffer with 10 mM digitonin [µL]	0	0	0	0	0	0	0	0	0	45

After mixing with digitonin the samples were incubated for 4 min at RT, and then centrifuged immediately at 14000 x *g*, RT for 2 min. 200 µL of the supernatant were collected and mixed with 50 µL 5x Sample buffer and boiled for 5 min. The samples were stored at -20°C until they were run on SDS-PAGE and analyzed by Western blot.

Fractionation and Western blot analysis were performed with the help of Michala Boudová.

3.6 SDS-PAGE

SDS-PAGE was used for assessment of expression of the v5-tagged cell lines and fractionation experiments and done according to Laemmli protocol [87]. The separation gel was 12% acrylamide, 375 mM Tris-HCl, pH 8.8 and 0.1% (w/v) SDS. The stacking gel was made of 5% acrylamide, 125mM Tris-HCl, pH 6.8, and 0.1% (w/v) SDS. Polymerization

was induced by adding 0.1% (w/v) ammonium persulfate and 0.025% (v/v) TEMED for the separation gel, and 0.1% (w/v) ammonium persulfate and 0.005% (v/v) TEMED for the stacking gel. As running buffer 25 mM Tris, 192 mM glycine and 0.1% (w/v) SDS was used. The gel was run at 75 V until the sample migrated into the separation gel and was then run at 125 V until completion. As molecular weight marker the Precisions Plus Protein^{TM} Dual Color Standards (Bio-Rad) was used.

For checking of the expression of v5-tagged cell lines, $5x10^7$ cells of mid-log culture were harvested by centrifugation (1000 x *g*, RT, 10 min) and washed once with PBS and resuspended in PBS to a concentration of $1x10^9$ cells/mL. An appropriate amount of 5x SDS-Sample buffer (5xSB) was added and the sample was boiled at 98°C for 10 min. 12.5 µL of sample corresponding to $1x10^7$ cells were loaded per lane on a 12% SDS-PAGE gel.

For the digitonin fractionation a volume corresponding to $1x10^7$ cells was loaded on the gel per well.

For analysis of the pull-down of the v5-tagged proteins samples were run on a 15 well Bolt^{TM} 4-12% Bis-Tris Plus gel (ThermoFisher scientific, NW04125BOX) using NuPAGE® MES SDS Running Buffer (ThermoFisher scientific, NP0002) at 125 V.

3.6.1 Western blot analysis

For visualization of specific protein bands by immunostaining proteins separated on SDS-PAGE gels were transferred onto PVDF membranes by wet electro blotting. PVDF membrane was activated by immersing it in pure methanol for 5 min. The proteins were blotted for 100 V using a Towbin buffer with SDS (25 mM Tris, 386 mM glycine, 3.7 g/L SDS, 20% (v/v) methanol).

After blotting, membranes were blocked in 5% milk in PBS-T for 1 hour at RT or at 4°C over night. According to protein of interest, primary antibodies were prepared at appropriate dilutions (Table 8) in 5% milk in PBS-T and applied on the membranes for 2 hours at RT and agitation. Table 8 summarizes the antibodies used for analysis of the digitonin gradient fractionation by Western blot.

After application of the primary antibody, membranes were washed 3 times with PBS-T. Secondary antibodies were applied diluted in 5% (w/v) milk in PBS-T according to

dilutions shown in Table 8, for 1 hour at RT and agitation. The final wash was performed with 5 times 5 min with 5 mL PBS-T. For visualization the membranes were incubated for 1 min with Clarity™ Western ECL (Bio-Rad) and pictures were recorded on a ChemiDoc MP (Bio-Rad) using the Image Lab™ software. Pictures were exported for analysis from the Image Lab software and analyzed and manipulated using Fiji [85] and Irfanview.

Table 8: Used primary and secondary antibodies for western blot analysis, protein used to use raise the antibody in which organism, dilution used in western blot analysis, size of the corresponding protein in *T. brucei*, source of the antibody. The observed size of the v5 antibody depends on the tagged protein.

Antibody(Protein)	**Organism**	**Dilution**	**Size**	**Source**
TbEnolase	Rabbit	1:2000	55.7 kDa	Paul Michels, University of Edinburgh
TbLa	Rabbit	1:1000	37.7 kDa	[84]
TbErv1	Rabbit	1:1000	30.4 kDa	[88]
TbHsp70	Mouse	1:1000	70 kDa	[89]
V5 Epitope Tag	Mouse	1:1000	various	ThermoFisher scientific, 37-7500
Secondary antibodies				
Anti-Mouse IgG peroxidase antibody		rabbit	1:2000	Sigma-Aldrich, A9044
Anti-Rabbit IgG peroxidase antibody		goat	1:1000	Sigma-Aldrich, A0545

3.6.2 Gel staining

For general visualization of proteins on SDS-PAGE gels, gels were treated with SYPRO® Ruby Protein Gel Stain (ThermoFisher scientific, S-12000) or for more sensitive staining Silver staining was applied using the SilverQuest™ Silver Staining Kit (ThermoFisher scientific, LC6070). Both Kits were applied following the provided manuals.

3.7 Co-Immunoprecipitation

3.7.1 Preparation of anti-v5 antibody coated Dynabeads®

For performing of the co-immunoprecipitation first the beads had to be loaded with the antibody. It was chosen to covalently link the antibody to epoxy beads to avoid unwanted elution of antibody from the beads in the final elution step, as the heavy chain of the antibody has similar size as one of the proteins of interest.

All solutions used for preparation and handling of Dynabeads® were prepared with MiliQ water and filtered through a 0.22 µm filter before use.

For preparation of the beads, 10 mg Dynabeads® M-270 Epoxy (ThermoFisher scientific, 14302D) were washed with 1 mL 100 mM Na-phosphate, pH 7.4, for 15 min at RT. The pre-wetted beads were mixed with the 200 µL of the anti-v5 antibody (V5 epitope tag, ThermoFisher scientific, 37-7500, 0.5 mg protein/mL) and 100 µL 3M $(NH_4)_2SO_4$ and incubated for 48 hours at 30°C under constant rotating. After the incubation period the beads were washed 5 min each with 100 mM Na-phosphate, pH7.4; 100 mM glycine, pH 2.5; 100 mM Tris-HCl, pH 8.8; 100 mM triethylamine; 2xPBS; PBS + 0.5% (v/v) TX-100 and 1xPBS, in the order stated. The glycine and triethylamine wash was only performed for 30 sec. After the last wash the beads were resuspended in 50 µL 1xPBS (50 µ/10 mg beads) and stored at 4°C until use.

3.7.2 Pull-down using Cryogrinding

For cryogrinding, $1x10^9$ cells of mid-log v5-taagged cells were harvested by spinning them at 1000 x *g*, 4°C for 10 min. The cells were washed once with 5 mL PBS, resuspended in 500 µL PBS and transferred to a 1.5 mL microcentrifuge tube. They were spun for 3 min at 1800 x *g* and the supernatant was removed so the remaining solution including the cell pellet made up for a total of 100 µL. The cells were resuspended in the remaining volume of PBS and then fast-frozen by dropping them directly into liquid nitrogen. The frozen cells were stored at -80°C until they were processed.

For cryogenic grinding a CryoGrinder (OPS Diagnostic) was precooled in nitrogen vapors over a bath of liquid nitrogen. Cryomilling was performed for 15-20 min, and assessed under the microscope for homogeneity. If insufficient defragmentation of the cells was observed, grinding was continued for additional 5 min. This was performed until 80-90% of cells were broken. The cell powder was stored at -80°C until use for pull-downs.

For the pull-downs, the cell powder was resuspended in 500 µL lysis buffer (20 mM HEPES, pH 7.4, 150 mM Na-Citrate, 1 mM $MgCl_2$, 0.1 mM $CaCl_2$, 0.1% (v/v) TX-100, + cOmplete™, EDTA free protein inhibitor (1 tablet per 10 mL buffer)) and centrifuged for 10 min at 20000 x *g*, 6°C. The clear lysate was collected and added to 3 µL of the v5-antibody coated Dynabeads. The suspension was incubated for 2 hours at 4°C and agitation. After the incubation the beads were collected magnetically and washed 4 times 5 min with 1 mL of the lysis buffer. The washed beads were incubated at 72°C for 10 min with 100 µL elution buffer (25 mM Tris-HCl, pH 7.5, 2% (w/v) SDS), and the eluate was collected. An aliquot was taken for western blot analysis and silver staining and the

remaining amount was ethanol precipitated. The protein pellet was stored at -80°C and was sent for proteomic analysis by Mass Spectrometry to Brno (Proteomic Core Facility and Research Group Proteomic, CEITEC-MU, Masaryk University, Brno).

As negative control, and as control for the protein identification by mass spectrometry, untagged SmOxP9 was processed the same way as the tagged cell lines.

3.7.3 Pull-down using total Lysis

For a simple pull-down cells were processed similar as in the procedure with cryogrinding, except that cells were not plunged frozen and ground, but lysed by adding 2 mL lysis buffer .5TX (20 mM HEPES, pH 7.4, 150 mM Na-Citrate, 1 mM $MgCl_2$, 0.1 mM $CaCl_2$, 0.5% (v/v) TX-100, + cOmplete™, EDTA free protein inhibitor (1 tablet per 10 mL buffer)) per $3x10^9$ cells and incubation for 5 min on ice. After lysing, the suspension was spun for 20 min at 20000 x *g*, 8°C. The supernatant was collected and added to 6 µL of the bead suspension. After incubating for 2 hours at 4°C and agitation, the beads were washed 4X 5 min with 1 mL lysis buffer without Triton X-100. The elution and further steps were carried out as described for the pull-down with cryogrinding.

3.8 Aconitase Activity measurement

For measurements of aconitase activity, cells were fractionated into crude cytosolic and mitochondrial fraction, similar to the procedure described in section 3.4 Crude cellular fractionation but using a buffer optimized for aconitase stability [90].

The cell lines 29-13, TbCia2A+TbCia2B-RNAi, TbCia1+TbCia2B-RNAi were grown in 100 mL in SDM-79 to densities between $0.5\text{-}1x10^7$ cells/mL and the RNAi cell lines were induced for 3 and 6 days. $5x10^8$ cells of each cell line were harvested by centrifugation at 1000 x *g*, 4°C for 10 min. The cell pellet was washed twice with ice-cold lysis buffer (25 mM Tris-HCl, pH 7.6, 225 mM Sucrose, 2 mM EDTA, 2 mM EGTA, 10 mM KH_2PO_4, 1 mM $MgSO_4$, 10 mM Na-Citrate, 2 mM Dithiotreitol (DTT), + cOmplete™, EDTA free protein inhibitor (1 tablet per 10 mL buffer)) and resuspended in 500 µL of the lysis buffer and kept on ice. Citrate and DTT was added to enhance the stability of aconitase [90]. 400 µL of the cell suspension were mixed with a sufficient amount of digitonin (10 mg/mL in MiliQ) to reach a final concentration of 0.4 mg/mL digitonin. The suspension was vortexed for a few seconds and incubated for 5 min at 25°C (RT). After spinning for 2 min at 14000 x *g* and RT, the supernatant representing the cytosolic fraction was collected and

placed on ice for later use, for longer storage it was placed into a -20°C freezer. The pellet obtained from the centrifugation was washed once with activity buffer and then resuspended in fresh 400 µL activity buffer. It was mixed with Triton X-100 a final concentration of 0.1% (v/v) TX-100 and incubated for 5 min on ice. The remaining 100 µL of the cell suspension were washed once with PBS and resuspended in 500 µL MiliQ water. 10 µL of this suspension was used for protein concentration measurement by the Bradford protein assay.

For measuring of the aconitase activity 10 µL of lysate were diluted to 250 µL with activity buffer and DL-isocitric acid trisodium salt solution, to obtain a final concentration of 10 mM DL-isocitrate in a 84.6 mM Tris buffer with pH 7.5. The mixtures were prepared in replicas of three in a 96 well plate with UV transmissible bottom, and over a time course of 10 min the change in absorbance at 240 nm was measured on an Infinite® M200 PRO (Tecan). The change in absorbance corresponds to the increase of aconitate. Assuming Lambert beers law and an independence of the molar extinction coefficient of aconitate from its concentration [90], the rise of absorbance was normalized with the measured protein concentration of the 100 µL cells suspension aliquot by the Bradford assay. Activities of non-induced cells were compared relative to induced cells.

4 Results and discussion

4.1 Tagging of TbCia1, TbMms19, TbCia2A, and TbCia2B with 3xV5

Four cell lines were successfully generated from the parental cell line SMOXP9 expressing an endogenously c-terminal V5 tagged version of TbCia1, TbMms19, TbCia2A or TbCia2B. After selection of positive clones with hygromycin, expression of the tagged proteins was confirmed by western blot analysis using a monoclonal α-v5 antibody (Figure 6).

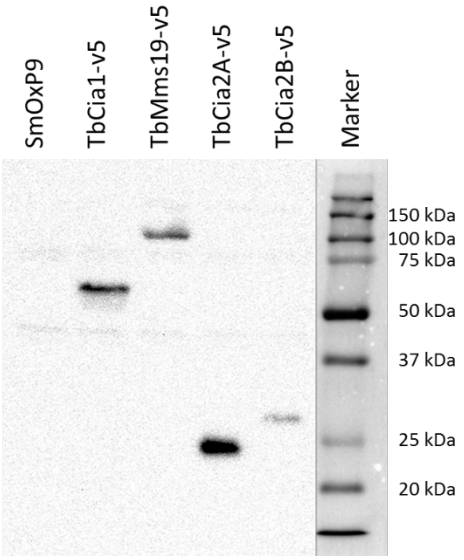

Figure 6: Western blot showing the expression of the v5-tagged cell lines, parental (SmOxP9) cell line as control, $0.5x10^6$ cells/lane, anti-v5 antibody, dilution 1:1000

Table 9: Sizes of the v5-tagged proteins

Protein	Size (with tag)
TbCia1-v5	52.5 kDa
TbMms19-v5	109.6 kDa
TbCia2A-v5	22.5 kDa
TbCia2B-v5	23.8 kDa

The size of the expressed protein corresponded to that of the predicted one (Table 9). The intensity of the bands displays the expression of the proteins relative to each other. According to the expression profile, TbCia2A is more abundant than TbCia2B; in case their role would be redundant, TbCia2A still takes up a higher percentage of their function than TbCia2B. If any of the components would be found strictly in a complex with other components, it would be assumed that they are expressed in the ratios in which they would be present in such complex [26]. There is however no obvious pattern which can be observed. Assuming 1:1 ratios and TbCia1 as scaffold in each of the suggested sub-

complexes, the intensities could make up for one complex with TbMms19 as well as one with TbCia2B. TbCia2A is present in excess so it might have some other function additional to its function in Fe-S cluster loading.

4.2 Localization

Studies in yeast, human, plants and other organisms showed that the homologues of the studied proteins are localized in to cytosol and some also to the nucleus [64][65][74][91]. Two independent approaches (IFA and digitonin fractionation) were used to investigate if the *T. brucei* proteins are localized in the cytosol as required to take part in the cytosolic iron-sulfur cluster assembly.

4.2.1 Localization by IFA

The v5-tagged cells were prepared for IFA, with MitoTracker as mitochondrial marker, and with α-TbEnolase antibody as a marker for the cytosol. DAPI was used to stain DNA within the cell therefore serving as marker for nucleus and kinetoplast. The tagged proteins were detected using monoclonal α-v5 antibody.

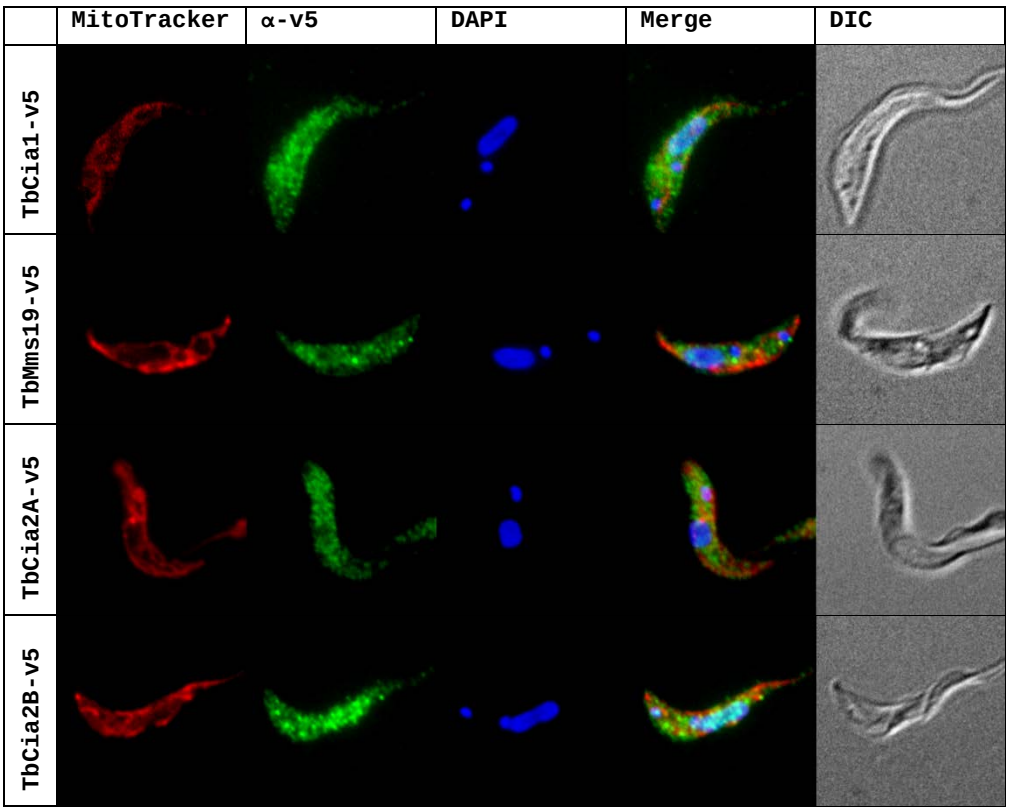

Figure 7: IFA of representative cells for the v5-tagged cell lines, MitoTracker in red as mitochondrial marker, protein of interest in green, DAPI in blue as DNA marker

All four proteins display a cytosolic distribution as already reported for homologues of these proteins in other organisms. None of them co-localizes with the mitochondrion.

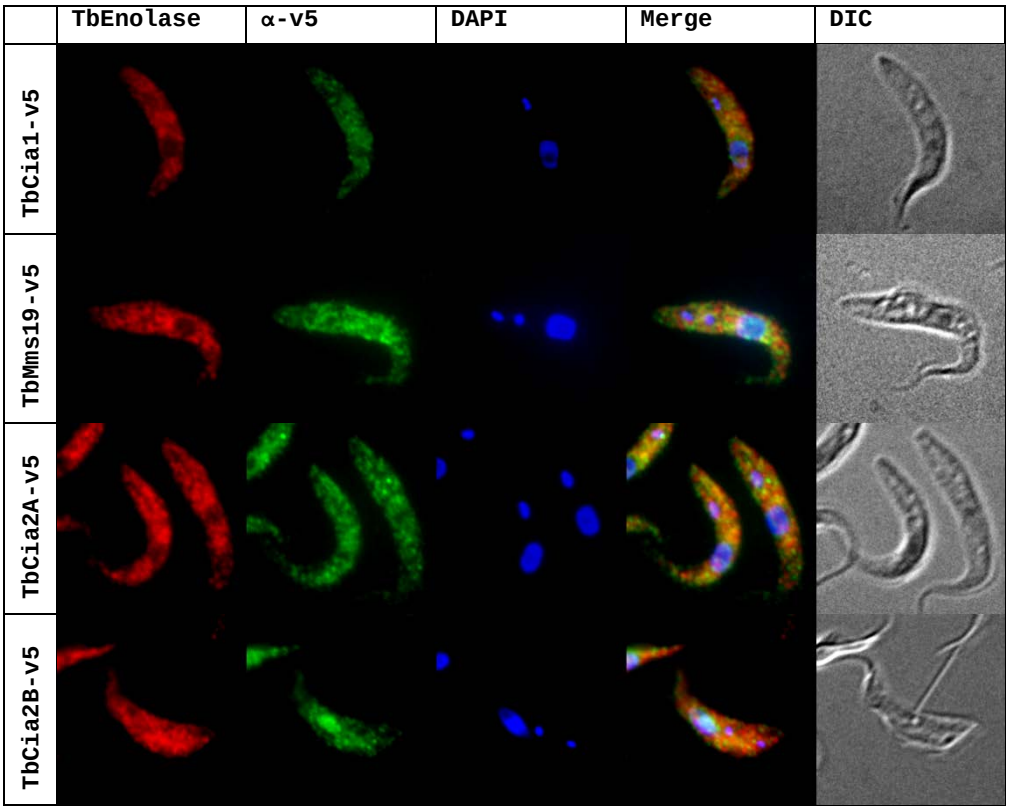

Figure 8: IFA of representative cells for the v5-tagged cell lines, TbEnolase in red as cytosolic marker, protein of interest in green, DAPI in blue as DNA marker

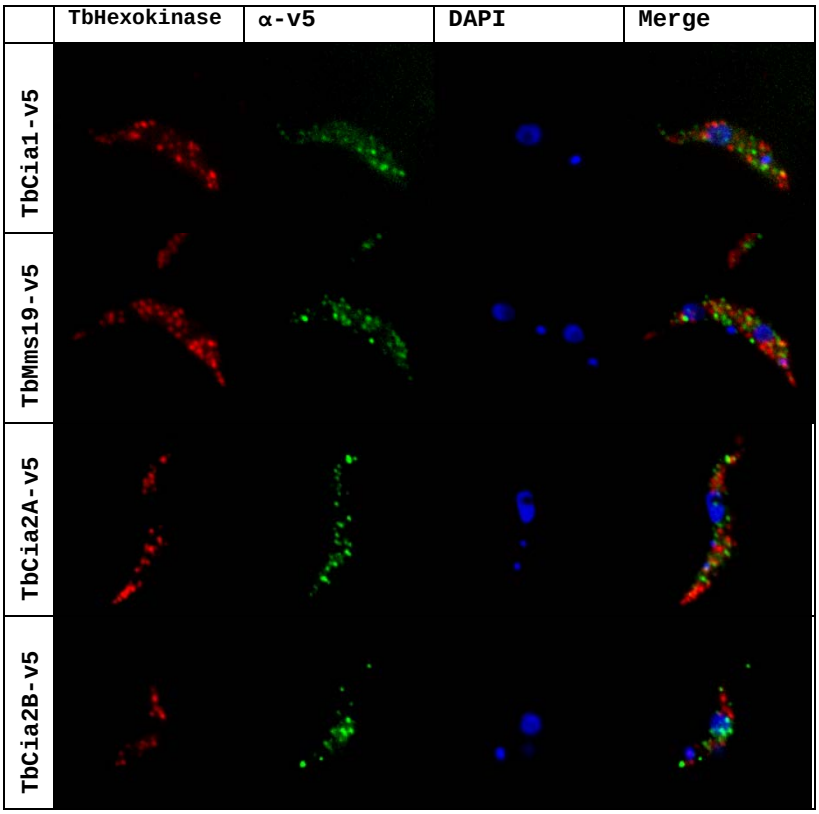

Figure 9: IFA of representative cells for the v5-tagged cell-lines. TbHexokinase in red as glycosomal marker, proteins of interest in green, DAPI in blue as DNA marker

The proteins, although they are widely distributed over the cytosol, show a distinct distribution as clustered foci, indicating that they may be part of larger complexes. This would be expected from pathways which require more proteins to be localized at the same place to increase speed and efficiency of substrate processing [92]. As the size of the foci was similar to glycosomes in *T. brucei*, IFA using the glycosomal marker TbHexokinase was performed to rule out this possibility. Figure 9 shows that neither of the proteins colocalizes with the glycosomes.

Additionally to its cytosolic localization, TbCia2B showed a strong signal co-localizing with the nucleus. As it cannot be distinguished by simple fluorescence microscopy if the signal is coming from within the nucleus or if the protein is located around the nucleus or in the nuclear envelope, TbCia2B-v5 cells were also analyzed by confocal microscopy. The nuclear envelope was ruled out, as none of the here studied proteins was found in a published *T. brucei* nuclear envelope proteome [93]. A study in human showed that FAM96B is interacting with prelamin A which targets to the nuclear envelope and to nucleus[74]. However, *Trypanosoma* do not possess a gene coding for prelamin.

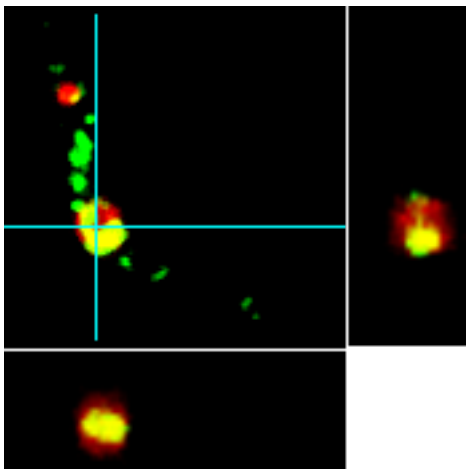

Figure 10: Confocal image of TbCia2B-v5, protein of interest in green, DAPI in red, blue lines indicate orthoslices through the XZ and the XY plane of the z-stack, which are shown beside the image

For confocal microscopy a z-stack was recorded to be able to differentiate clearly if the signal is coming from within the nucleus or from a localization close to the nuclear envelope. Figure 10 shows one confocal plane of a representative cell, including orthoslices through the XZ and the XY plane of the z-stack. A clear co-localization of the protein with part of the DAPI signal in the nucleus was observed, suggesting that the protein has a dual localization, in both nucleus and cytosol. The protein resides in 2-3 distinct foci within the nucleus. The role of TbCia2B in the nucleus remains to be elucidated.

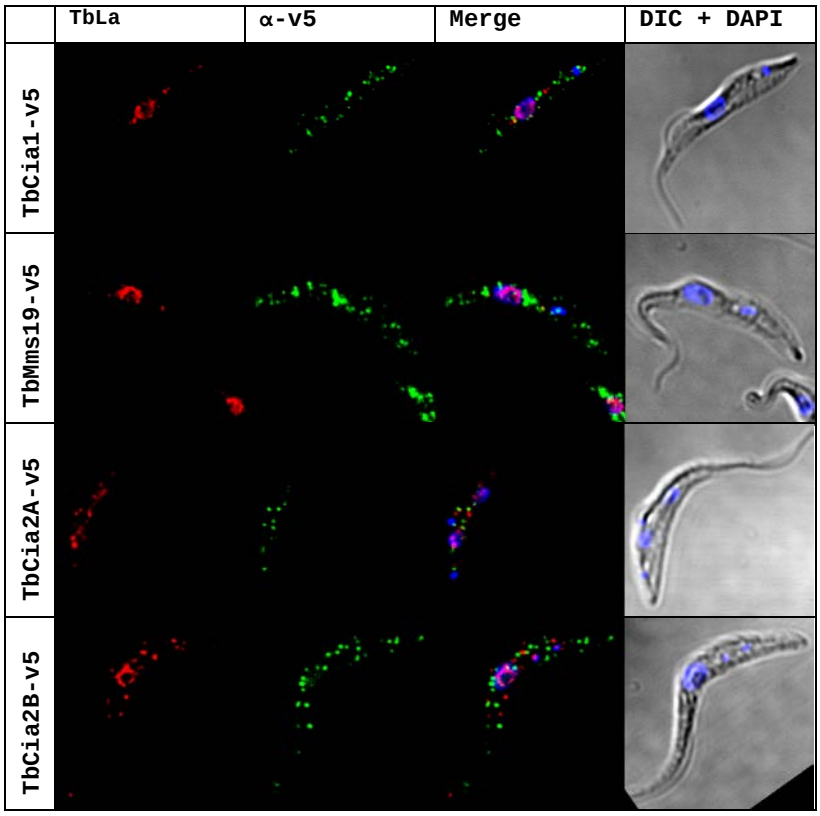

Figure 11: Confocal images of representative cells for the v5-tagged cell-lines using sequential illumination. TbLa in red as nuclear marker, proteins of interest in green, DAPI in blue as DNA marker

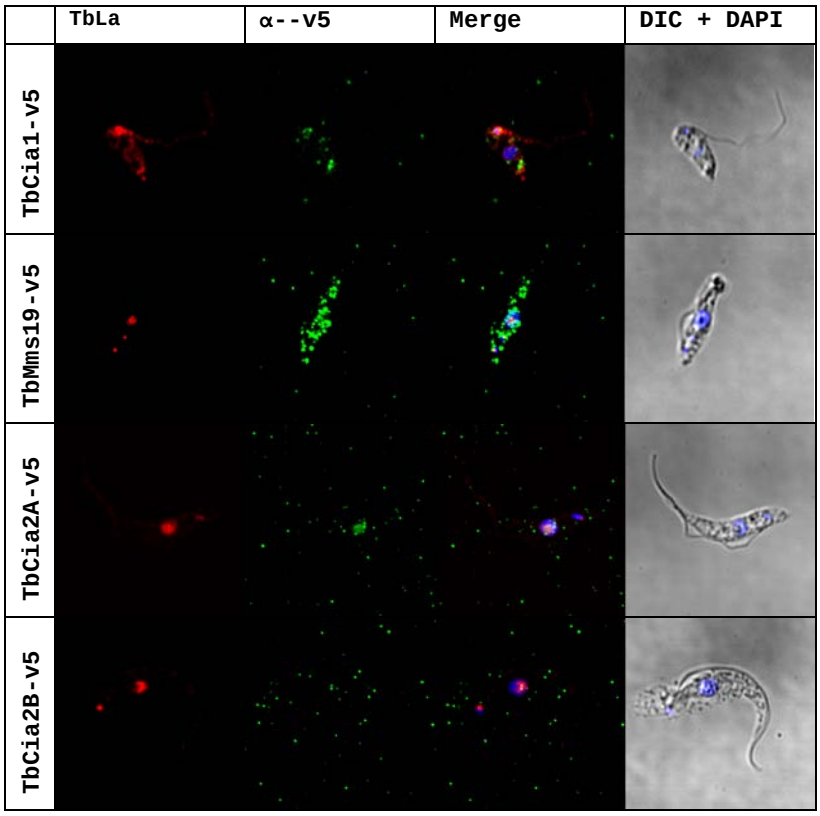

Figure 12: Confocal images of NP-40 treated v5-tagged cell-lines using sequential illumination. TbLa in red as nuclear marker, proteins of interest in green, DAPI in blue as DNA marker

To determine if TbCia2B or any of the other proteins were interacting with DNA the cells were treated with NP-40 prior to fixation [94], and IFAs were prepared using α-TbLa antibody as nuclear marker [84]. Figure 11 shows confocal images of cells treated with α-v5 and α-TbLa antibody. Figure 12 shows confocal images of cell treated with NP-40.

NP-40 permeabilizes membranes but leaves intact interactions of proteins with DNA [94]. None of the proteins seem to interact directly with DNA as in the NP-40 treated cells, the signal in the nucleus is weakened. However, it was quite evident from NP-40 treated cells that the proteins are part of very stable complexes, as they remained visible after the detergent extraction, supposing that part of them would be released from the cellular matrix by the treatment. Initially observed with the classic IFA treatment, these foci were considered artifacts or unspecific binding to dirt particles. This hypothesis was ruled out with the NP40 treatment, as the observed foci were observed only in the detergent-treated cells expressing the tagged proteins and not in cells untreated (Figure 11) nor in parental cell lines (data not shown).

4.2.2 Localization by cellular fractionation

As additional control for the cytosolic localization of the v5-tagged proteins, cells were crudely fractionated to obtain a cytosolic and an organellar fraction. The used concentration of digitonin partially releases nuclear proteins, and it was therefore not suitable for TbCia2B to differentiate the nuclear from the cytosolic fraction. This could however be achieved by a digitonin gradient experiment or by ultracentrifugation, in which the nucleus could be separated from the cytosol, as well as from other organelles.

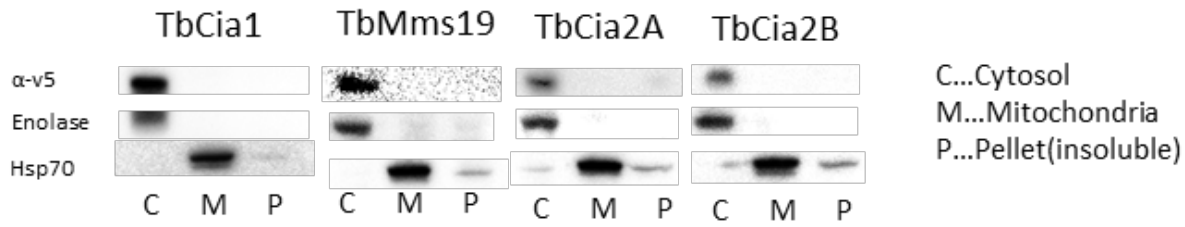

Figure 13: Crude fractionation of cytosol from mitochondria by digitonin for the v5 tagged cell lines, tagged proteins detected with anti-v5 antibody, enolase as cytosolic marker, Hsp70 as mitochondrial marker

The pellet contains membrane and DNA bound proteins as well as insoluble proteins. The fractionation (Figure 13) showed that none of the tagged proteins is insoluble, so the tag does not impair their solubility nor leads to a missfolding, which could lead to aggregation. All of the proteins show same localization as enolase giving another independent experiment showing that they are cytosolic. The fractionation shows that none of the studied proteins

shows mitochondrial localization and they are not impaired in their solubility because of the addition of the C-terminal v5-tag, so they can be used for the pull-down experiment.

To get further insight into the localization of TbCia2B, I performed a selective permeabilization of whole cells with digitonin for an independent assay on and test the dual localization. TbCia2B-v5 cells were therefore exposed to different concentrations of digitonin ranging from 0.05 to 1.5 mM digitonin and the obtained lysates were analyzed by Western blot. As nuclear marker α-TbLa protein was used [84], as cytosolic marker enolase, for mitochondria α-TbmtHsp70 and α-TbErv1for mitochondrial intermembrane space [88]. The result is shown in Figure 14.

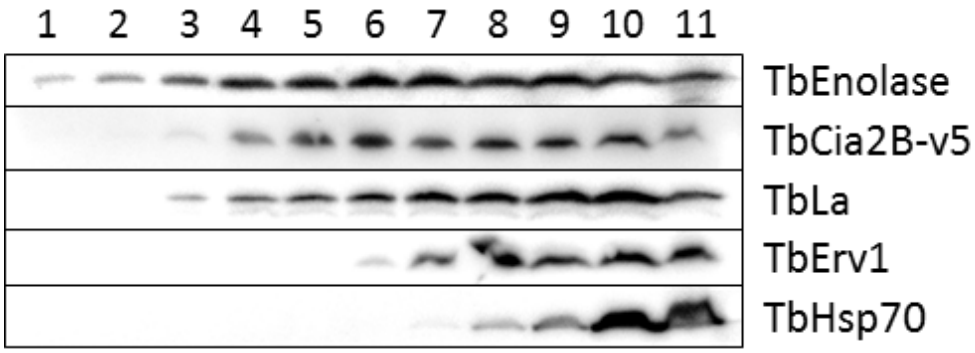

Figure 14: Selective permeabilization of whole TbCia2B-v5 cells, lane 1-10: increasing digitonin concentrations from 0 to 1.5 mM, lane 11: whole cell lysate

The intensities of the western signals were quantified using Fiji [85] and normalized to the highest intensity observed in any of the measured fractions (Figure 15).

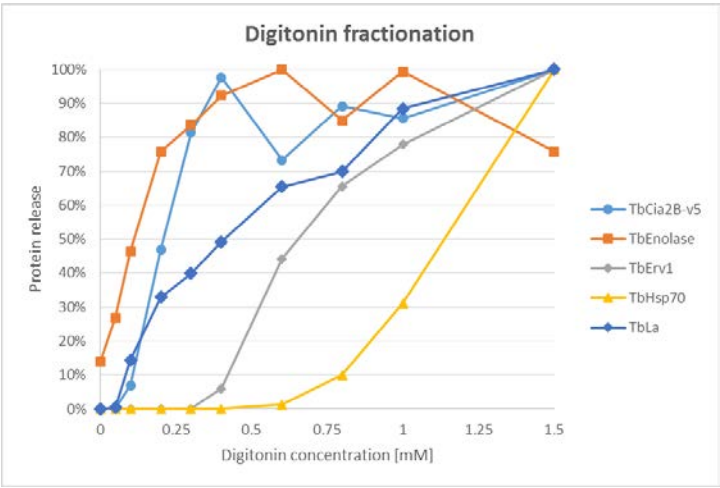

Figure 15: Quantification of digitonin gradient fractionation of TbCia2B-v5 cells

The fractionation showed that TbCia2B-v5 is released later than the cytosolic marker enolase but it is released prior to TbLa, the nuclear marker; this release pattern may originate

from a combination of cytosolic and nuclear localization. The faster release from the nucleus is an indicative of a less strong interaction within the organelle, which may result from a lack of association with DNA, a result in agreement with the IFA after detergent extraction. Overall, the release of TbCia2B-v5 indicates the protein is more soluble than TbLa, despite their presence in the same organelle. Overall this experiment confirms the dual localization of TbCia2B-v5 in cytosol and nucleus as observed by the immunofluorescence assays.

4.2.3 Summary of localization experiments

Concluding from the localization experiments by immunostaining and by the digitonin fractionation I can say that all four studied proteins TbCia1, TbMms19, TbCia2A and TbCia2B are localized in the cytosol of *T. brucei*, and TbCia2B is additionally localized in the nucleus. All tagged proteins are soluble and are not localizing neither to the mitochondrion nor the glycosome, and they are not binding DNA. They show a distinct accumulation in foci within the cytosol indicating that they form complexes, stable enough even in conditions that would allow cytosolic matrix to be released, as shown in the NP-40 experiment. TbCia2B also forms foci within the nucleus, where it may also function in a complex; however probably not with the other CIA targeting components herein studied. A proper functional characterization of TbCia2B is still required to define the rule of TbCia2B in the nucleus [95]. That TbCia1, TbMms19 or TbCia2A are also localized to the nucleus cannot be completely ruled out as they might be present at very low concentrations, below the detection limit of the chosen IFA method. A strong localization of TbCia1 as observed for yeast Cia1 is definitely not the case in *T. brucei* [64]. The crude cellular fractionation could be optimized to separate cytosolic from the other fractions including nucleus, and might result in a pattern as observed in *Arabidopsis thaliana* where Cia1, Mms19, Cia2 and even Nar1 partially localize to the nucleus [75]. Some proteins require a nuclear localization signal (NLS) to be translocated into this organelle. The NLS is usually rich in arginine (R) and lysine (K), frequently encountered as quadruplet or combinations of doublets and quadruplets spaced by random amino acids [96]. Little is known about the NLS of *T. brucei* and it seems to behave substantially different from those in mammalian cells, as software trained to detect human NLSs is not able to detect experimentally determined NLSs in *T. brucei* [97]. Assuming similar requirements for the NLS in trypanosomes as in other eukaryotes, the localization of TbCia2B may result from a n-terminal quadruplet containing the sequence KRKR which might be sufficient for nuclear import [96]. In a previous attempt to tag TbCia2B with eYFP, live cell imaging also showed a partial localization to the

nucleus but only for the c-terminal tagged version. The n-terminal eYFP tagged TbCia2B did not localize to the nucleus (data not shown). The eYFP tagged version however was only transiently transfected and the cells lost the signal within a few weeks, probably due to an incompatibility with the tag, which may have interfered with the function of the protein. The observation that only the c-terminal tagged protein was able be translocated to the nucleus confirms the importance of the n-terminus of TbCia2B for nuclear import. A blast search conducted on UniProtKD [98] and alignment of the obtained hits suggested that the KRKR motif seems to be unique for *T. brucei brucei* and *T. brucei gambiense*, and is not even conserved to other close related species found in the database.

4.3 Co-Immunoprecipitation

All tagged proteins were purified by co-immunoprecipitation for the determination of their interacting partners or substrates. Previous tagging of the proteins with PTP resulted in an unsuccessful pull-down, probably because of the high time requirement of the 2-step PTP pull-down procedure. Therefore it was chosen to use a smaller tag for a 1-step purification with Dynabeads.

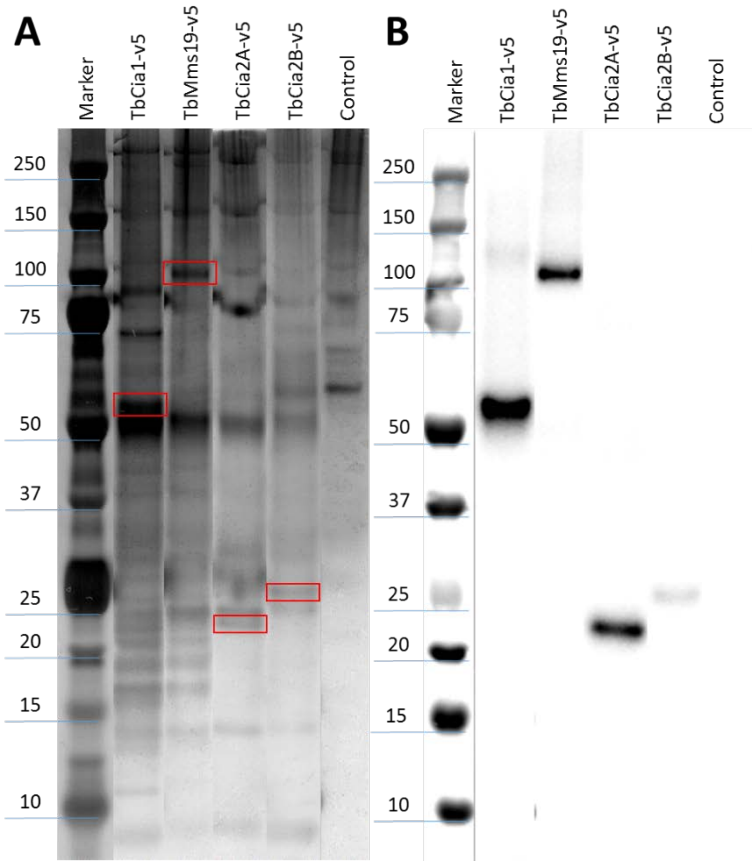

Figure 16: A - Silver staining, the baits used for the pull downs are marked within the red bars, **B** – Western blot using anti-v5 antibody

To be able to use mild lysis conditions with a low detergent buffer the cells were ground to powder at liquid nitrogen temperatures, and the resuspended powder was used for the pull-down, allowing shorter times of purification after preparation of cell suspension. A fraction of the eluate was analyzed by Western blot assay and silver staining, while the rest was used for protein identification by mass spectrometry. The western blot (Figure 16B) confirms that the tagged proteins of correct size were pulled down. The same bands are also visible in silver stained SDS-PAGE (Figure 16A), and are absent from the negative control pull-down (Figure 16, lane 6: control). The silver stained SDS-gel shows several bands resulting from unspecific binding of proteins to the beads, which will be edited out of the MS results when comparing the samples with the control sample.

4.4 Aconitase activity measurements

Aconitase is a well-known Fe-S protein. The cluster in aconitase is required for its enzymatic activity, as it stabilizes the carbonyl group of the citrate withdrawing electron density, allowing the water to be removed to form aconitate [14]. Aconitase in *T. brucei* has a dual localization in cytosol and mitochondrion, while being encoded by only one gene [90]. In the mitochondrion it performs its known function in the TCA cycle, while its function in the cytosol is unclear. In human, the apo-form of aconitase is called IRP2 (iron regulatory protein 2), which may bind RNA and influences the transcription of proteins involved in the uptake of iron. In *T. brucei* no binding of apo-aconitase to RNA or its involvement in iron homeostasis has been reported. Nevertheless the cytosolic aconitase obtains a Fe-S cluster over the CIA pathway, therefore the measurement of cytosolic aconitase activity may be used as indicator for the impairment of the CIA pathway, as already reported in previous publications of this laboratory [32][78].

The current model for the targeting of Fe-S clusters in the cytosol is facilitated by various sub-complexes. In humans, the delivery of the cluster onto IRP2 is solely facilitated by Cia2A (homologue of TbCia2A), which receives the cluster from IOP1 (TbNar1). It was already shown that knockdown of TbCia1 in *T. brucei* resulted in a decrease of c-aconitase activity [78]. As Cia1 is supposedly the scaffold protein involved in the assembly of most of the sub-complexes, the other late acting CIA components were also investigated for their influence on the c-aconitase activity upon knockdown to determine if they are also part of the complex that delivers the Fe-S cluster to c-aconitase.

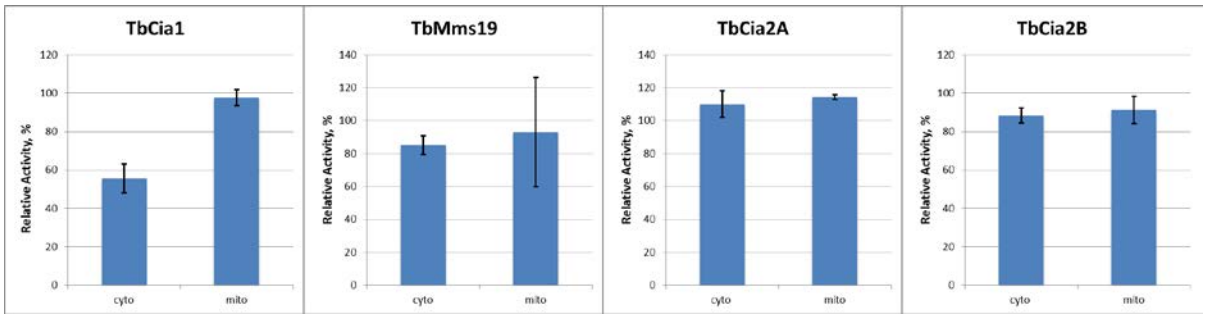

Figure 17: Aconitase activities for single RNAi knockdowns, activity shown as induced relative to non-induced, 6 days induction at point of measurement, error bars show 95% confidence interval, TbCia1 from [78], TbMms19 from Somsuvro Basu (unpublished data)

Apart from TbCia1, neither of the other late acting CIA components show a significant change in aconitase activity, whether in cytosol or in the mitochondrion (see Figure 17). Therefore, the double knock-down cell lines TbCia1+TbCia2B-RNAi and TbCia2A+TbCia2B-RNAi, which showed a growth phenotype that their single components did not, were analyzed for their influence on the aconitase activity upon induction.

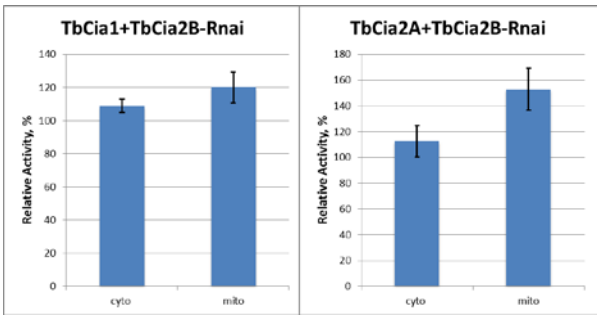

Figure 18: Aconitase activities for double RNAi knockdowns, activity shown as induced relative to non-induced, 6 days induction at point of measurement, error bars show 95% confidence interval

None of the two double knock-down cell lines show a decrease of c-aconitase activity upon induction. However, taking into account that the single knock-down for TbCia1 showed a decrease in c-aconitase of around 50%, this decrease was not observed by the additional knockdown of TbCia2B. This may result from a lower RNAi efficiency for TbCia1 in the double knockdown compared to the single. Both show an incomplete down regulation of TbCia1 by Western blot analysis [78][unpublished data], but it cannot be judged without proper quantification of the knockdown efficiency if the same level of depletion was achieved. The possibility cannot be ruled out that TbCia1 was not downregulated enough in the knock-down to observe an effect on c-aconitase activity. Assuming a sufficient depletion of TbCia1 necessary for an observable decrease in aconitase activity, but a recovery of the effect through the parallel knockdown of TbCia2B, several scenarios might be the case. If TbCia2B has a negative regulating role on the cluster transfer by TbCia1, we would expect an upregulation of c-aconitase activity in the single knockdown

of TbCia2B, which we did not. This still could be the case if TbCia2B can be functionally replaced by TbCia2A. Another option could be that the absence of TbCia1 and TbCia2B leads to the recruitment of a second cytosolic cluster delivery pathway, other than the CIA, for the maturation of c-aconitase. This recruitment would be initiated by the absence of TbCia2B alone, as the knock-down of early acting CIA components showed decrease of c-aconitase active, consistent with the proposed requirement of the CIA pathway for the maturation of c-aconitase [78].

Recent studies in human showed that the cancer related protein NEET can receive a [2Fe-2S] cluster from the mitochondrial ISC and transfer it to Dre2, as well as use it to repair the cluster on c-aconitase (IRP1). Although NEET could not complement the CIA pathway, as it cannot assemble clusters on GPAT or IOP1, it may repair c-aconitase, which lost its cluster by oxidative stress. *In vitro* NEET was also able to assemble a [4Fe-4S] cluster onto c-aconitase by interconversion of its [2Fe-2S] cluster [99][100]. Although *T. brucei* possesses no homologue of NEET identifiable by blast, the findings in humans demonstrate that the export of ready-assembled clusters from the mitochondria and interconversion of [2Fe-2S] clusters is possible [99]. There may be another Fe-S cluster export machinery in *T brucei*, which becomes activated if TbCia2B is down regulated, and allows reconstitution of c-aconitase. Also the question of the cluster assembly of the [2Fe-2S] cluster on Dre2 and the bridging [4Fe-4S] cluster on the Cfd1-Nbp35 scaffold remains unanswered, so the possibility of an auxiliary cluster assembly machinery, for the formation of [2Fe-2S] clusters as well as [4Fe-4S] cluster remains to be investigated.

The TbCia2A+TbCia2B-RNAi cell line shows no effect on c-aconitase activity, but instead this activity is upregulated in the mitochondrion. This is in contrast with the observation made in the TbCia1+TbCia2B RNAi, where if adequate depletion is assumed, it suggests that TbCia2B does have a role in regulation of c- aconitase. The upregulation of mitochondrial aconitase was an unexpected result for it is assumed that the maturation of mitochondrial aconitase is independent of the CIA, and the ISC pathway should perform this role in the mitochondrion. Moreover, it is unknown how the distribution of aconitase between the cytosol and mitochondrion is regulated, so it is difficult to depict a model on how the depletion of both TbCia2A and TbCia2B cause an upregulation of mitochondrial aconitase activity. It may be also possible that aconitase obtains its cluster in the mitochondria and the mature protein is then transported back to the cytosol. A further understanding of the actual function of aconitase in the cytosol of *T. brucei* and the

regulation of its distribution between cytosol and mitochondrion would be useful to understand the finding made with the knock-down of the CIA targeting components.

5 Conclusions

All components (TbCia1, TbMms19, TbCia2A and TbCia2B) of the cytosolic iron-sulfur cluster assembly targeting machinery were successfully and stable endogenously c-terminally tagged with 3x v5-tag in the procyclic stage of *T. brucei*. The tagged proteins were expressed in the newly generated cell lines and used for localization studies as well as for co-immunoprecipitation experiments.

The tagged proteins exhibit cytosolic localization while forming distinct foci, which may be required for them to perform their expected function, targeting Fe-S clusters from the CIA machinery to apoproteins. TbCia2B additionally localizes to the nucleus, as confirmed by IFA and selective permeabilization of whole cells with digitonin. None of the proteins was found to be present neither in the mitochondrion nor in glycosomes. Their distinctive differential expression and different localization pattern suggests that TbCia2A and TbCia2B probably do not have a redundant function, but together they do not seem to be involved in the maturation of c-aconitase, as indicated by the aconitase activity assays on their double knock-down. On the other hand, a double knock-down of TbCia1 and TbCia2B shows no decrease on cytosolic aconitase, although a single knock-down of TbCia1 does [78]. The parallel knock down of TbCia2B can therefore rescue the knock-down effect of TbCia1. Without further data it is difficult to discern the role and function of TbCia2B in the maturation of c-aconitase and it should be further investigated. C-aconitase showed not to be useful as a control for the functionality of the CIA targeting complex, for it seems to require only part of the CIA targeting components. More Fe-S cluster proteins should be investigated for their enzymatic activity upon depletion of individual CIA targeting components. Nevertheless this finding once again raised the curiosity about the function of c-aconitase and I suggest this protein should be further investigated, especially because my findings suggest existence of a possible parallel machinery involved in the maturation of aconitase in the cytosol.

6 References

[1] J. Lukeš and S. Basu, “Fe/S protein biogenesis in trypanosomes — A review,” *Biochim. Biophys. Acta - Mol. Cell Res.*, vol. 1853, no. 6, pp. 1481–1492, 2015.

[2] V. Hampl, L. Hug, J. W. Leigh, J. B. Dacks, B. F. Lang, A. G. B. Simpson, and A. J. Roger, “Phylogenomic analyses support the monophyly of Excavata and resolve relationships among eukaryotic ‘supergroups’.,” *Proc. Natl. Acad. Sci. U. S. A.*, vol. 106, no. 10, pp. 3859–64, 2009.

[3] F. Bringaud, L. Rivière, and V. Coustou, “Energy metabolism of trypanosomatids: adaptation to available carbon sources.,” *Mol. Biochem. Parasitol.*, vol. 149, no. 1, pp. 1–9, Oct. 2006.

[4] D. Montagnes, E. Roberts, J. Lukeš, and C. Lowe, “The rise of model protozoa.,” *Trends Microbiol.*, vol. 20, no. 4, pp. 184–91, Apr. 2012.

[5] R. Lill, M. Ulrich, and U. Mühlenhoff, “Maturation of iron-sulfur proteins in eukaryotes: mechanisms, connected processes, and diseases.,” *Annu. Rev. Biochem.*, vol. 77, pp. 669–700, Jan. 2008.

[6] N. Tanaka, M. Kanazawa, K. Tonosaki, N. Yokoyama, T. Kuzuyama, and Y. Takahashi, “Novel features of the ISC machinery revealed by characterization of Escherichia coli mutants that survive without iron-sulfur clusters.,” *Mol. Microbiol.*, Nov. 2015.

[7] X. M. Xu and S. G. Møller, “Iron-sulfur clusters: biogenesis, molecular mechanisms, and their functional significance.,” *Antioxid. Redox Signal.*, vol. 15, no. 1, pp. 271–307, Jul. 2011.

[8] H. Beinert, R. H. Holm, and E. Mu, “Iron-Sulfur Clusters : Nature ’ s Modular , Multipurpose Structures,” *Science (80-.).*, vol. 277, no. August, pp. 653–659, 1997.

[9] J. W. Peters, M. H. B. Stowell, S. M. Soltis, M. G. Finnegan, M. K. Johnson, and D. C. Rees, “Redox-dependent structural changes in the nitrogenase P-cluster,” *Biochemistry*, vol. 36, no. 6, pp. 1181–1187, 1997.

[10] G. Wächtershäuser, “Groundworks for an evolutionary biochemistry: the iron-sulphur world.,” *Prog. Biophys. Mol. Biol.*, vol. 58, no. 2, pp. 85–201, Jan. 1992.

[11] M. Rivas, A. Becerra, J. Peretó, J. L. Bada, and A. Lazcano, “Metalloproteins and the pyrite-based origin of life: a critical assessment.,” *Orig. Life Evol. Biosph.*, vol. 41, no. 4, pp. 347–56, 2011.

[12] H. Beinert, J. Meyer, and R. Lill, *Iron-Sulfur Proteins*. Elsevier, 2004.

[13] R. Lill, “Function and biogenesis of iron-sulphur proteins.,” *Nature*, vol. 460, no. 7257, pp. 831–8, Aug. 2009.

[14] S. J. Lloyd, H. Lauble, G. S. Prasad, and C. D. Stout, “The mechanism of aconitase: 1.8 A resolution crystal structure of the S642a:citrate complex.,” *Protein Sci.*, vol. 8, no. 12, pp. 2655–62, Dec. 1999.

[15] R. H. Sands and H. Beinert, “Studies on mitochondria and submitochondrial particles by paramagnetic resonance (EPR) spectroscopy,” *Biochem. Biophys. Res. Commun.*,

vol. 3, no. 1, pp. 47–52, Jul. 1960.

[16] D. V. DerVartanian, W. H. Orme-Johnson, R. E. Hansen, H. Beinert, R. L. Tsai, J. C. M. Tsibris, R. C. Bartholomaus, and I. C. Gunsalus, “Identification of sulfur as component of the EPR signal at g = 1.94 by isotopic substitution,” *Biochem. Biophys. Res. Commun.*, vol. 26, no. 5, pp. 569–576, Mar. 1967.

[17] J. Meyer, “Iron–sulfur protein folds, iron–sulfur chemistry, and evolution,” *J. Biol. Inorg. Chem.*, vol. 13, no. 2, pp. 157–170, 2008.

[18] R. Lill, R. Dutkiewicz, H.-P. Elsässer, A. Hausmann, D. J. a Netz, A. J. Pierik, O. Stehling, E. Urzica, and U. Mühlenhoff, “Mechanisms of iron-sulfur protein maturation in mitochondria, cytosol and nucleus of eukaryotes.,” *Biochim. Biophys. Acta*, vol. 1763, no. 7, pp. 652–67, Jul. 2006.

[19] D. Schneider, K. Jaschkowitz, A. Seidler, and M. Rögner, “Overexpression and reconstitution of a Rieske iron-sulfur protein from the cyanobacterium Synechocystis PCC 6803.,” *Indian J. Biochem. Biophys.*, vol. 37, no. 6, pp. 441–6, Dec. 2000.

[20] R. Malkin and J. C. Rabinowitz, “The reconstitution of clostridial ferredoxin,” *Biochem. Biophys. Res. Commun.*, vol. 23, no. 6, pp. 822–827, Jun. 1966.

[21] E. C. Raulfs, I. P. O. Carroll, P. C. Dos Santos, M. Unciuleac, D. R. Dean, I. P. O’Carroll, and P. C. Dos Santos, “In vivo iron-sulfur cluster formation.,” *Proc. Natl. Acad. Sci. U. S. A.*, vol. 105, no. 25, pp. 8591–6, Jun. 2008.

[22] D. C. Johnson, D. R. Dean, A. D. Smith, and M. K. Johnson, “Structure, function, and formation of biological iron-sulfur clusters.,” *Annu. Rev. Biochem.*, vol. 74, pp. 247–81, Jan. 2005.

[23] R. Lill and U. Mühlenhoff, “Iron-sulfur protein biogenesis in eukaryotes: components and mechanisms.,” *Annu. Rev. Cell Dev. Biol.*, vol. 22, pp. 457–86, Jan. 2006.

[24] J. Balk and S. Lobréaux, “Biogenesis of iron-sulfur proteins in plants,” *Trends Plant Sci.*, vol. 10, no. 7, pp. 324–331, 2005.

[25] A. K. Sharma, L. J. Pallesen, R. J. Spang, and W. E. Walden, “Cytosolic iron-sulfur cluster assembly (CIA) system: factors, mechanism, and relevance to cellular iron regulation.,” *J. Biol. Chem.*, vol. 285, no. 35, pp. 26745–51, Aug. 2010.

[26] V. D. Paul and R. Lill, “Biogenesis of cytosolic and nuclear iron–sulfur proteins and their role in genome stability,” *Biochim. Biophys. Acta - Mol. Cell Res.*, vol. 1853, no. 6, pp. 1528–1539, 2015.

[27] L. Zheng, R. H. White, V. L. Cash, R. F. Jack, and D. R. Dean, “Cysteine desulfurase activity indicates a role for NIFS in metallocluster biosynthesis.,” *Proc. Natl. Acad. Sci. U. S. A.*, vol. 90, no. April, pp. 2754–2758, 1993.

[28] L. Zheng, V. L. Cash, D. H. Flint, and D. R. Dean, “Assembly of Iron-Sulfur Clusters: IDENTIFICATION OF AN iscSUA-hscBA-fdx GENE CLUSTER FROM AZOTOBACTER VINELANDII,” *J. Biol. Chem.*, vol. 273, no. 21, pp. 13264–13272, May 1998.

[29] F. Barras, L. Loiseau, and B. Py, “How Escherichia coli and Saccharomyces cerevisiae Build Fe/S Proteins,” *Adv. Microb. Physiol.*, vol. 50, pp. 41–101, 2005.

[30] A. P. G. Frazzon, M. V Ramirez, U. Warek, J. Balk, J. Frazzon, D. R. Dean, and B. S. J. Winkel, “Functional analysis of Arabidopsis genes involved in mitochondrial iron-sulfur cluster assembly.,” *Plant Mol. Biol.*, vol. 64, no. 3, pp. 225–40, Jun. 2007.

[31] W.-H. Tong and T. Rouault, “Distinct iron-sulfur cluster assembly complexes exist in the cytosol and mitochondria of human cells.,” *Eur. Mol. Biol. Organ. J.*, vol. 19, no. 21, pp. 5692–5700, 2000.

[32] O. Smíd, E. Horákova, V. Vilímova, I. Hrdy, R. Cammack, A. Horváth, J. Lukes, and J. Tachezy, “Knock-downs of iron-sulfur cluster assembly proteins IscS and IscU down-regulate the active mitochondrion of procyclic Trypanosoma brucei,” *J. Biol. Chem.*, vol. 281, no. 39, pp. 28679–28686, 2006.

[33] J. Tovar, G. León-Avila, L. B. Sánchez, R. Sutak, J. Tachezy, M. van der Giezen, M. Hernández, M. Müller, and J. M. Lucocq, “Mitochondrial remnant organelles of Giardia function in iron-sulphur protein maturation.,” *Nature*, vol. 426, no. 6963, pp. 172–176, 2003.

[34] S. Bandyopadhyay, K. Chandramouli, and M. K. Johnson, “Iron-sulfur cluster biosynthesis.,” *Biochem. Soc. Trans.*, vol. 36, no. Pt 6, pp. 1112–9, 2008.

[35] A. Pandey, H. Yoon, E. R. Lyver, A. Dancis, and D. Pain, “Identification of a Nfs1p-bound persulfide intermediate in Fe-S cluster synthesis by intact mitochondria.,” *Mitochondrion*, vol. 12, pp. 539–549, Jul. 2012.

[36] A. C. Adam, C. Bornhövd, H. Prokisch, W. Neupert, and K. Hell, “The Nfs1 interacting protein Isd11 has an essential role in Fe/S cluster biogenesis in mitochondria.,” *EMBO J.*, vol. 25, no. 1, pp. 174–83, Jan. 2006.

[37] F. Foury and T. Roganti, “Deletion of the mitochondrial carrier genes MRS3 and MRS4 suppresses mitochondrial iron accumulation in a yeast frataxin-deficient strain,” *J. Biol. Chem.*, vol. 277, no. 27, pp. 24475–24483, 2002.

[38] F. Colin, A. Martelli, M. Clémancey, J. M. Latour, S. Gambarelli, L. Zeppieri, C. Birck, A. Page, H. Puccio, and S. Ollagnier De Choudens, “Mammalian frataxin controls sulfur production and iron entry during de novo Fe4S4 cluster assembly,” *J. Am. Chem. Soc.*, vol. 135, pp. 733–740, 2013.

[39] O. Stehling and R. Lill, “The role of mitochondria in cellular iron-sulfur protein biogenesis: mechanisms, connected processes, and diseases.,” *Cold Spring Harb. Perspect. Biol.*, vol. 5, no. 8, p. a011312–, Jan. 2013.

[40] R. Yan, S. Adinolfi, and A. Pastore, “Ferredoxin, in conjunction with NADPH and ferredoxin-NADP reductase, transfers electrons to the IscS/IscU complex to promote iron-sulfur cluster assembly.,” *Biochim. Biophys. Acta*, Feb. 2015.

[41] M. a Uzarska, R. Dutkiewicz, S.-A. Freibert, R. Lill, and U. Mühlenhoff, “The mitochondrial Hsp70 chaperone Ssq1 facilitates Fe/S cluster transfer from Isu1 to Grx5 by complex formation.,” *Mol. Biol. Cell*, vol. 24, no. 12, pp. 1830–41, 2013.

[42] V. D. Paul and R. Lill, “SnapShot: Eukaryotic Fe-S Protein Biogenesis.,” *Cell Metab.*, vol. 20, no. 2, pp. 384–384.e1, Aug. 2014.

[43] L. Banci, D. Brancaccio, S. Ciofi-Baffoni, R. Del Conte, R. Gadepalli, M. Mikolajczyk, S. Neri, M. Piccioli, and J. Winkelmann, “[2Fe-2S] cluster transfer in

iron-sulfur protein biogenesis," *Proc. Natl. Acad. Sci.*, vol. 111, no. 17, pp. 6203–6208, Apr. 2014.

[44] A. D. Sheftel, C. Wilbrecht, O. Stehling, B. Niggemeyer, H.-P. Elsässer, U. Mühlenhoff, and R. Lill, "The human mitochondrial ISCA1, ISCA2, and IBA57 proteins are required for [4Fe-4S] protein maturation.," *Mol. Biol. Cell*, vol. 23, no. 7, pp. 1157–66, 2012.

[45] D. Brancaccio, A. Gallo, M. Mikolajczyk, K. Zovo, P. Palumaa, E. Novellino, M. Piccioli, S. Ciofi-Baffoni, and L. Banci, "Formation of [4Fe-4S] Clusters in the Mitochondrial Iron–Sulfur Cluster Assembly Machinery," *J. Am. Chem. Soc.*, vol. 136, no. 46, pp. 16240–16250, 2014.

[46] G. Kispal, P. Csere, C. Prohl, and R. Lill, "The mitochondrial proteins Atm1p and Nfs1p are essential for biogenesis of cytosolic Fe/S proteins.," *EMBO J.*, vol. 18, no. 14, pp. 3981–9, Jul. 1999.

[47] D. J. a Netz, M. Stümpfig, C. Doré, U. Mühlenhoff, A. J. Pierik, and R. Lill, "Tah18 transfers electrons to Dre2 in cytosolic iron-sulfur protein biogenesis.," *Nat. Chem. Biol.*, vol. 6, no. 10, pp. 758–65, Oct. 2010.

[48] A. D. Tsaousis, E. Gentekaki, L. Eme, D. Gaston, and A. J. Roger, "Evolution of the Cytosolic Iron-Sulfur Cluster Assembly Machinery in Blastocystis Species and Other Microbial Eukaryotes," *Eukaryot. Cell*, vol. 13, no. 1, pp. 143–153, 2014.

[49] L. J. Pallesen, N. Solodovnikova, A. K. Sharma, and W. E. Walden, "Interaction with Cfd1 Increases the Kinetic Lability of FeS on the Nbp35 Scaffold," *J. Biol. Chem.*, vol. 288, no. 32, pp. 23358–67, Jun. 2013.

[50] H. Kohbushi, Y. Nakai, S. Kikuchi, and T. Yabe, "Arabidopsis cytosolic Nbp35 homodimer can assemble both and clusters in two distinct domains," *Biochem. …*, vol. 378, no. 4, pp. 810–815, 2009.

[51] D. J. A. Netz, A. J. Pierik, M. Stümpfig, E. Bill, A. K. Sharma, L. J. Pallesen, W. E. Walden, and R. Lill, "A bridging [4Fe-4S] cluster and nucleotide binding are essential for function of the Cfd1-Nbp35 complex as a scaffold in iron-sulfur protein maturation.," *J. Biol. Chem.*, vol. 287, no. 15, pp. 12365–78, Apr. 2012.

[52] E. J. Camire, J. D. Grossman, G. J. Thole, N. M. Fleischman, and D. L. Perlstein, "The Yeast Nbp35-Cfd1 Cytosolic Iron-Sulfur Cluster Scaffold Is an ATPase.," *J. Biol. Chem.*, vol. 290, no. 39, pp. 23793–802, Sep. 2015.

[53] R. Lill, R. Dutkiewicz, S. a. Freibert, T. Heidenreich, J. Mascarenhas, D. J. Netz, V. D. Paul, A. J. Pierik, N. Richter, M. Stümpfig, V. Srinivasan, O. Stehling, and U. Mühlenhoff, "The role of mitochondria and the CIA machinery in the maturation of cytosolic and nuclear iron–sulfur proteins," *Eur. J. Cell Biol.*, vol. 94, no. 7–9, pp. 280–291, 2015.

[54] H. Lange, T. Lisowsky, J. Gerber, U. Mühlenhoff, G. Kispal, and R. Lill, "An essential function of the mitochondrial sulfhydryl oxidase Erv1p/ALR in the maturation of cytosolic Fe/S proteins," *EMBO Rep.*, vol. 2, no. 8, pp. 715–720, 2001.

[55] H. K. Ozer, A. C. Dlouhy, J. D. Thornton, J. Hu, Y. Liu, J. J. Barycki, J. Balk, and C. E. Outten, "Cytosolic Fe-S Cluster Protein Maturation and Iron Regulation Are Independent of the Mitochondrial Erv1/Mia40 Import System," *J. Biol. Chem.*, vol.

290, no. 46, pp. 27829–27850, 2015.

[56] L. Vernis, C. Facca, E. Delagoutte, N. Soler, R. Chanet, B. Guiard, G. Faye, and G. Baldacci, “A newly identified essential complex, Dre2-Tah18, controls mitochondria integrity and cell death after oxidative stress in yeast.,” *PLoS One*, vol. 4, no. 2, p. e4376, Jan. 2009.

[57] N. Soler, C. T. Craescu, J. Gallay, Y.-M. M. Frapart, D. Mansuy, B. Raynal, G. Baldacci, A. Pastore, M.-E. E. Huang, and L. Vernis, “A S-adenosylmethionine methyltransferase-like domain within the essential, Fe-S-containing yeast protein Dre2.,” *FEBS J.*, vol. 279, no. 12, pp. 2108–19, Jun. 2012.

[58] Y. Zhang, E. R. Lyver, E. Nakamaru-Ogiso, H. Yoon, B. Amutha, D.-W. Lee, E. Bi, T. Ohnishi, F. Daldal, D. Pain, and A. Dancis, “Dre2, a conserved eukaryotic Fe/S cluster protein, functions in cytosolic Fe/S protein biogenesis.,” *Mol. Cell. Biol.*, vol. 28, no. 18, pp. 5569–82, Sep. 2008.

[59] L. Banci, I. Bertini, V. Calderone, S. Ciofi-Baffoni, A. Giachetti, D. Jaiswal, M. Mikolajczyk, M. Piccioli, and J. Winkelmann, “Molecular view of an electron transfer process essential for iron-sulfur protein biogenesis.,” *Proc. Natl. Acad. Sci. U. S. A.*, vol. 110, no. 18, pp. 7136–41, 2013.

[60] U. Mühlenhoff, S. Molik, J. R. Godoy, M. A. Uzarska, N. Richter, A. Seubert, Y. Zhang, J. Stubbe, F. Pierrel, E. Herrero, C. H. Lillig, and R. Lill, “Cytosolic Monothiol Glutaredoxins Function in Intracellular Iron Sensing and Trafficking via Their Bound Iron-Sulfur Cluster,” *Cell Metab.*, vol. 12, no. 4, pp. 373–385, 2010.

[61] A. Hausmann, D. J. Aguilar Netz, J. Balk, A. J. Pierik, U. Mühlenhoff, and R. Lill, “The eukaryotic P loop NTPase Nbp35: an essential component of the cytosolic and nuclear iron-sulfur protein assembly machinery.,” *Proc. Natl. Acad. Sci. U. S. A.*, vol. 102, no. 9, pp. 3266–71, Mar. 2005.

[62] J. Balk, A. J. Pierik, D. J. A. Netz, U. Mühlenhoff, and R. Lill, “The hydrogenase-like Nar1p is essential for maturation of cytosolic and nuclear iron-sulphur proteins.,” *EMBO J.*, vol. 23, no. 10, pp. 2105–15, May 2004.

[63] M. Seki, Y. Takeda, K. Iwai, and K. Tanaka, “IOP1 protein is an external component of the human cytosolic iron-sulfur cluster assembly (CIA) machinery and functions in the MMS19 protein-dependent CIA pathway.,” *J. Biol. Chem.*, vol. 288, no. 23, pp. 16680–9, Jun. 2013.

[64] J. Balk, D. Netz, and K. Tepper, “The essential WD40 protein Cia1 is involved in a late step of cytosolic and nuclear iron-sulfur protein assembly,” *Mol. Cell. …*, vol. 25, no. 24, pp. 10833–10841, 2005.

[65] N. Van Wietmarschen, A. Moradian, G. B. Morin, P. M. Lansdorp, and E.-J. J. Uringa, “The mammalian proteins MMS19, MIP18, and ANT2 are involved in cytoplasmic iron-sulfur cluster protein assembly,” *J. Biol. Chem.*, vol. 287, no. 52, pp. 43351–43358, Nov. 2012.

[66] O. Stehling, J. Mascarenhas, A. a. Vashisht, A. D. Sheftel, B. Niggemeyer, R. Rösser, A. J. Pierik, J. a. Wohlschlegel, and R. Lill, “Human CIA2A-FAM96A and CIA2B-FAM96B integrate iron homeostasis and maturation of different subsets of cytosolic-nuclear iron-sulfur proteins,” *Cell Metab.*, vol. 18, no. 2, pp. 187–198, Jul. 2013.

[67] O. Stehling, A. a Vashisht, J. Mascarenhas, Z. O. Jonsson, T. Sharma, D. J. a Netz, A. J. Pierik, J. a Wohlschlegel, and R. Lill, “MMS19 assembles iron-sulfur proteins required for DNA metabolism and genomic integrity.,” *Science*, vol. 337, no. 6091, pp. 195–9, Jul. 2012.

[68] E. Weerapana, C. Wang, G. M. Simon, F. Richter, S. Khare, M. B. D. Dillon, D. A. Bachovchin, K. Mowen, D. Baker, and B. F. Cravatt, “Quantitative reactivity profiling predicts functional cysteines in proteomes.,” *Nature*, vol. 468, no. 7325, pp. 790–5, Dec. 2010.

[69] I. Lev, M. Volpe, L. Goor, N. Levinton, L. Emuna, and S. Ben-Aroya, “Reverse PCA, a Systematic Approach for Identifying Genes Important for the Physical Interaction between Protein Pairs,” *PLoS Genet.*, vol. 9, no. 10, pp. 1–13, 2013.

[70] S. Lauder, M. Bankmann, S. N. Guzder, P. Sung, L. Prakash, and S. Prakash, “Dual requirement for the yeast MMS19 gene in DNA repair and RNA polymerase II transcription.,” *Mol. Cell. Biol.*, vol. 16, no. 12, pp. 6783–93, 1996.

[71] L. Queimado, M. Rao, R. A. Schultz, E. V Koonin, L. Aravind, T. Nardo, M. Stefanini, and E. C. Friedberg, “Cloning the human and mouse MMS19 genes and functional complementation of a yeast mms19 deletion mutant.,” *Nucleic Acids Res.*, vol. 29, no. 9, pp. 1884–1891, 2001.

[72] T. Seroz, G. S. Winkler, J. Auriol, R. a Verhage, W. Vermeulen, B. Smit, J. Brouwer, a P. Eker, G. Weeda, J. M. Egly, and J. H. Hoeijmakers, “Cloning of a human homolog of the yeast nucleotide excision repair gene MMS19 and interaction with transcription repair factor TFIIH via the XPB and XPD helicases.,” *Nucleic Acids Res.*, vol. 28, no. 22, pp. 4506–13, Nov. 2000.

[73] K. Gari, A. M. L. Ortiz, V. Borel, H. Flynn, J. M. Skehel, and S. J. Boulton, “MMS19 Links Cytoplasmic Iron-Sulfur Cluster Assembly to DNA Metabolism.,” *Science*, vol. 243, no. June, pp. 1–12, Jun. 2012.

[74] X. Xiong, J. Wang, H. Zheng, X. Jing, Z. Liu, Z. Zhou, and X. Liu, “Identification of FAM96B as a novel prelamin A binding partner.,” *Biochem. Biophys. Res. Commun.*, vol. 440, no. 1, pp. 6–10, 2013.

[75] Y.-F. Han, H.-W. Huang, L. Li, T. Cai, S. Chen, and X.-J. He, “The Cytosolic Iron-Sulfur Cluster Assembly Protein MMS19 Regulates Transcriptional Gene Silencing, DNA Repair, and Flowering Time in Arabidopsis,” *PLoS One*, vol. 10, no. 6, p. e0129137, 2015.

[76] E. Horáková, P. Changmai, Z. Paris, D. Salmon, and J. Lukeš, “Simultaneous depletion of Atm and Mdl rebalances cytosolic Fe-S cluster assembly but not heme import into the mitochondrion of *Trypanosoma brucei*,” *FEBS J.*, vol. 282, no. 21, pp. 4157–4175, 2015.

[77] E. I. Bruske, F. Sendfeld, and A. Schneider, “Thiolated tRNAs of Trypanosoma brucei are imported into mitochondria and dethiolated after import,” *J. Biol. Chem.*, vol. 284, no. 52, pp. 36491–36499, 2009.

[78] S. Basu, D. J. Netz, A. C. Haindrich, N. Herlerth, T. J. Lagny, A. J. Pierik, R. Lill, and J. Lukeš, “Cytosolic iron-sulphur protein assembly is functionally conserved and essential in procyclic and bloodstream Trypanosoma brucei.,” *Mol. Microbiol.*, vol. 93, no. 5, pp. 897–910, Sep. 2014.

[79] E. Wirtz, S. Leal, C. Ochatt, and G. a Cross, “A tightly regulated inducible expression system for conditional gene knock-outs and dominant-negative genetics in Trypanosoma brucei.,” *Mol. Biochem. Parasitol.*, vol. 99, no. 1, pp. 89–101, Mar. 1999.

[80] S. K. Poon, L. Peacock, W. Gibson, K. Gull, and S. Kelly, “A modular and optimized single marker system for generating Trypanosoma brucei cell lines expressing T7 RNA polymerase and the tetracycline repressor.,” *Open Biol.*, vol. 2, no. 2, p. 110037, Feb. 2012.

[81] R. Brun and Schönenberger, “Cultivation and in vitro cloning or procyclic culture forms of Trypanosoma brucei in a semi-defined medium. Short communication.,” *Acta Trop.*, vol. 36, pp. 289–292, 1979.

[82] S. Dean, J. Sunter, R. J. Wheeler, I. Hodkinson, E. Gluenz, K. Gull, and S. Dean, “A toolkit enabling efficient , scalable and reproducible gene tagging in trypanosomatids,” *Open Biol.*, 2015.

[83] S. V Sambasivarao, “NIH Public Access,” vol. 18, no. 9, pp. 1199–1216, 2013.

[84] S. Foldynová-Trantírková, Z. Paris, N. R. Sturm, D. a Campbell, and J. Lukes, “The Trypanosoma brucei La protein is a candidate poly(U) shield that impacts spliced leader RNA maturation and tRNA intron removal.,” *Int. J. Parasitol.*, vol. 35, no. 4, pp. 359–66, 2005.

[85] J. Schindelin, I. Arganda-Carreras, E. Frise, V. Kaynig, M. Longair, T. Pietzsch, S. Preibisch, C. Rueden, S. Saalfeld, B. Schmid, J.-Y. Tinevez, D. J. White, V. Hartenstein, K. Eliceiri, P. Tomancak, and A. Cardona, “Fiji: an open-source platform for biological-image analysis.,” *Nat. Methods*, vol. 9, no. 7, pp. 676–82, Jul. 2012.

[86] J. Moyersoen, J. Choe, A. Kumar, F. G. J. Voncken, W. G. J. Hol, and P. a M. Michels, “Characterization of Trypanosoma brucei/PEX14 and its role in the import of glycosomal matrix proteins,” *Eur. J. Biochem.*, vol. 270, no. 9, pp. 2059–2067, 2003.

[87] U. K. Laemmli, “Cleavage of structural proteins during the assembly of the head of bacteriophage T4.,” *Nature*, vol. 227, no. 5259, pp. 680–5, Aug. 1970.

[88] S. Basu, J. C. Leonard, N. Desai, D. A. I. Mavridou, K. H. Tang, A. D. Goddard, M. L. Ginger, J. Lukeš, and J. W. A. Allen, “Divergence of Erv1-associated mitochondrial import and export pathways in trypanosomes and anaerobic protists.,” *Eukaryot. Cell*, vol. 12, no. 2, pp. 343–55, Feb. 2013.

[89] A. K. Panigrahi, A. Zíková, R. a Dalley, N. Acestor, Y. Ogata, A. Anupama, P. J. Myler, and K. D. Stuart, “Mitochondrial complexes in Trypanosoma brucei: a novel complex and a unique oxidoreductase complex.,” *Mol. Cell. Proteomics*, vol. 7, no. 3, pp. 534–545, 2008.

[90] J. Saas, K. Ziegelbauer, A. Von Haeseler, B. Fast, and M. Boshart, “A developmentally regulated aconitase related to iron-regulatory protein-1 is localized in the cytoplasm and in the mitochondrion of Trypanosoma brucei,” *J. Biol. Chem.*, vol. 275, no. 4, pp. 2745–2755, 2000.

[91] C.-G. Duan, X. Wang, K. Tang, H. Zhang, S. K. Mangrauthia, M. Lei, C.-C. Hsu, Y.-J. Hou, C. Wang, Y. Li, W. A. Tao, and J.-K. Zhu, “MET18 Connects the Cytosolic

Iron-Sulfur Cluster Assembly Pathway to Active DNA Demethylation in Arabidopsis.," *PLoS Genet.*, vol. 11, no. 10, p. e1005559, 2015.

[92] M. Castellana, M. Z. Wilson, Y. Xu, P. Joshi, I. M. Cristea, J. D. Rabinowitz, Z. Gitai, and N. S. Wingreen, "Enzyme clustering accelerates processing of intermediates through metabolic channeling.," *Nat. Biotechnol.*, vol. 32, no. 10, pp. 1011–8, 2014.

[93] M. C. Field, V. Adung'a, S. Obado, B. T. Chait, and M. P. Rout, "Proteomics on the rims: insights into the biology of the nuclear envelope and flagellar pocket of trypanosomes.," *Parasitology*, vol. 139, no. 9, pp. 1158–67, Aug. 2012.

[94] J. Concepcion-Acevedo, J. Luo, and M. M. Klingbeil, "Dynamic Localization of Trypanosoma brucei Mitochondrial DNA Polymerase ID," *Eukaryot. Cell*, vol. 11, no. 7, pp. 844–855, 2012.

[95] R. Lill, "Only functional localization is faithful localization," vol. 1, no. 4, pp. 115–117, 2014.

[96] M. Marfori, A. Mynott, J. J. Ellis, A. M. Mehdi, N. F. W. Saunders, P. M. Curmi, J. K. Forwood, M. Bodén, and B. Kobe, "Molecular basis for specificity of nuclear import and prediction of nuclear localization," *Biochim. Biophys. Acta - Mol. Cell Res.*, vol. 1813, no. 9, pp. 1562–1577, 2011.

[97] M. S. Scott, P. V Troshin, and G. J. Barton, "NoD: a Nucleolar localization sequence detector for eukaryotic and viral proteins.," *BMC Bioinformatics*, vol. 12, no. 1, p. 317, 2011.

[98] T. U. Consortium, "UniProt: a hub for protein information," *Nucleic Acids Res.*, vol. 43, no. D1, pp. D204–D212, 2015.

[99] C. H. Lipper, M. L. Paddock, J. N. Onuchic, R. Mittler, R. Nechushtai, and P. A. Jennings, "Cancer-Related NEET Proteins Transfer 2Fe-2S Clusters to Anamorsin, a Protein Required for Cytosolic Iron-Sulfur Cluster Biogenesis," *PLoS One*, vol. 10, no. 10, p. e0139699, 2015.

[100] I. Ferecatu, S. Gonçalves, M.-P. Golinelli-Cohen, M. Clémancey, A. Martelli, S. Riquier, E. Guittet, J.-M. Latour, H. Puccio, J.-C. Drapier, E. Lescop, and C. Bouton, "The Diabetes Drug Target MitoNEET Governs a Novel Trafficking Pathway to Rebuild an Fe-S Cluster into Cytosolic Aconitase/Iron Regulatory Protein 1.," *J. Biol. Chem.*, vol. 289, no. 41, pp. 28070–28086, 2014.